放医研 図書室
8 0 1 9 9 6 0 1 3

NIRS

HIMAC

NIRS-M-110
HIMAC-010

放射線医学総合研究所図書館
8 10.24

Papers Contributed to the 10th Symposium on Accelerator Science and Technology

October 25-27, 1995
Hitachi-Naka

Edited by
Satoru Yamada
Masami Torikoshi

National Institute of Radiological Sciences
9-1, Anagawa 4-chome, Inageku, Chiba-shi 263, Japan

Foreword

Two years have passed since completion of HIMAC facility. During these two years, there have been many progress in the field of HIMAC operation, facility improvements, pre-clinical studies and clinical trials of heavy ion therapy. The most important thing to be emphasized among them is that the clinical trial has been successfully going on since June of 1994 using HIMAC. Many of these progress were reported at the 10th Symposium on Accelerator Science and Technology which was held in October 1995 at Hitachi-Naka.

As it seemed very significant to us that many people should know our efforts to bring the clinical trial of heavy ion therapy and the present status of HIMAC, we collected here the papers related to HIMAC which were presented at the above mentioned symposium. As most of the papers have been still under progressing, we will very appreciate your frank comments and criticisms.

Kiyomitsu Kawachi 河内清光
Director,
Division of Accelerator Physics and Engineering.

Contents

PHASE I/II CLINICAL TRIAL WITH HEAVY ION AT NATIONAL INSTITUTE OF RADIOLOGICAL SCIENCES

Kozo MORITA

Research Center of Charged Particle Therapy,
National Institute of radiological Sciences,
Chiba/Japan

In Japan the heavy particle therapy started already at NIRS in 1971. At first, the fast neutron beam was used inanticipation of its biological advantages. In some tumors, fast neutron therapy was more effective than conventional photon and electron therapy. But generally, the treatment results of fast neutron therapy were not satisfactory, because of its inadequate dose-distribution. Recently theproton beam with high energy is going to get into the spotlight. Its dose localization is excellent and the biological effect is almost the same as that of the photon beam. Therefore, radiation oncologists can easily become experi-enced in applying it to daily routine treatment.

High-LET charged particle radiotherapy has particular appeal for therapy of radioresistant neoplasms. The physical and biological properties secondary to heavy ions include, 1) advantageous dose localization at depth, 2) increased effect on hypoxic tumor cells by high-LET radia-tions, 3)less repair of sublethal and potentially lethal radiation damage, and 4) less variation of radioresponse in the different phases of the mitotic cell cycle. Since June last year our challenge has been to translate these theoretical advantages into significant clinical gains in the treatment of cancer. The objects of Phase I/II clinical trial using carbon-ion beam include the brain tumor, head and neck cancer, lung cancer, hepatoma, cervical cancerand cancer of the prostate. Fifty-five patients has been already treated. It takes long time to evaluate the usefulness of heavy ion therapy, because it is very importantto observe the treated patients at least several years after treatment. The preliminary results are encouraging. Although much has been learned regarding the potential of heavy charged particles, there is still a need for furtherresearch into their biology, physics and clinical applications.

PRESENT STATUS OF THE MEDICAL ACCELERATOR HIMAC

S. Yamada, N. Araki, M. Hosaka, A. Itano, M. Kanazawa, A. Kitagawa, T. Kohno**, M. Kumada, T. Murakami, M. Muramatsu, K. Noda, H. Ogawa, K. Sato***, S. Sato, Y. Sato, E. Takada, A. Tanaka, K. Tashiro, M. Torikoshi, J. Yoshizawa, T. Aoki*, T. Fukushima*, Y. Ishikawa*, T. Kimura*, R. Oishi*, K. Okumura*, Y. Sano*, Y. Sato*, T. Togashi* and K. Ueda*

Research Center of Charged Particle Therapy, National Institute of Radiological Sciences, 4-9-1 Anagawa, Inage-ku, Chiba 263

Abstract

Clinical study of cancer treatment has been going on since June 21, 1994 with HIMAC at NIRS. More than 50 patients have been treated with high energy carbon beams until August 4, 1995. The preliminary results look excellent as expected: very light damage on skin surface and remarkable effects on cancer cells.

HIMAC is operated day and night from 7 p.m. on Monday till 7 p.m. on Saturday for the clinical treatment and for basic experiments. About 1,500 hr. per year are used by clinical trials and 2,500 hr. is open for physical and biomedical users including researchers outside NIRS.

1. Introduction

Clinical trials and biomedical experiments at LBL[1] strongly suggest that the heavy ion therapy is very powerful especially in treating deeply seated tumors. The advantage of the therapy comes from the well known characteristics of heavy ions: a very good three dimensional dose localization in a human body. In a longitudinal dose distribution, a very sharp Bragg peak is observed around the end point of heavy ions. A high value of LET at the Bragg peak is also attractive in the treatment of radio-resistive tumors. Based on the long experience of radiotherapy with protons and fast neutrons, NIRS adopted heavy ion therapy because of these excellent characteristics of heavy ions.

The maximum energy of HIMAC is designed to be 800 MeV/u for light ions with q/A = 1/2 so that silicon ions reach 30 cm deep in water[2],[3]. Two ring structure of the main accelerator of HIMAC will allow further development of the beam quality and performance. Ion species ranging from He to Ar are required for the clinical treatment. In the facility, there are three treatment rooms one of which has both vertical and horizontal beam lines. The other two treatment rooms are equipped with a vertical and a horizontal beam lines, respectively.

2. Commissioning

The HIMAC project was approved in 1987 as one of the major project of "Comprehensive 10 year Strategy for Cancer Control" promoted by Japanese government since 1984. The first beam from the injector was obtained in late March 1993 with singly charged He ions. For the dual synchrotron rings, beam tests were begun in November 1993 with doubly charged He ions. The ions were accelerated to 230 MeV/u with a repetition rate of 1/2 Hz for each ring. Tests of the slow extraction from both rings were successfully completed in December and the extracted beams were transported to three treatment rooms within a few days. The length of the extracted beam spill was typically 300 ms.

After careful tuning of the accelerator system, biomedical and physical experiments were performed for a few months. Final check of the reliability of the total system was done with the carbon beam irradiation on a monkey. Clinical trials of the heavy ion cancer therapy started on June 21, 1994 with 290 MeV/u carbon ions. The first series of the treatment was successfully completed for three patients in August 1994. It takes about 90 seconds for a single fractional treatment, while the precise patient-positioning procedure requires about 20 min. Three treatments per week and total of 18 treatments for each patient were adopted as a protocol of the clinical trial.

The interim diagnosis shows excellent results: radiation damage on the mucous membrane seems very light in spite of the perfect damage of tumors. All of the first three patients got good recovery and already out of hospital. For some other patients, however, no remarkable improvements were observed.

In the second and the third series of the clinical trials, heavy ion treatment was applied to cancers at the head or neck, the lungs, the central nerve system, the uterus, the liver, the prostate *etc.* More than 50 patients are already treated with 290, 350 and 400 MeV/u

*Accelerator Engineering Corporation, 2-10-14, Konakadai, Inage-ku, Chiba 263.

**Present Address: Department of Energy Science, Tokyo Institute of Technology, 4259 Nagatsuda, Yokohama 226.

***Present Address: Research Center for Nuclear Physics, Osaka University, 10-1 Mihogaoka, Ibaraki, Osaka 567.

carbon ions. Total of 100 patients will be finished by the end of the fiscal year 1995.

3. Operation of HIMAC

In the early stage of the accelerator operation, all devices were turned off over night except for the vacuum system and the control system. After turning on in the morning, it took only 4 hr. to get the accelerated beam in a treatment room. Most part of the time are spent in tuning of the ion source and LEBT elements. After October 1994, HIMAC is operated day and night from Monday 7 p.m. to Saturday 7 p.m. In the day time of every Monday, weekly maintenance is scheduled. Accelerator Engineering Corporation (AEC) is responsible for the machine operation and the weekly maintenance. Major activities of the accelerator group of NIRS are set toward the improvements of the beam performance.

The machine time from 9 a.m. to 7 p.m. of the weekday is scheduled for the clinical trials and from 7 p.m. to the next 7 a.m. is open for users with carbon ions. From Friday 7 p.m. to Saturday 8 p.m., various kind of ion species are accelerated for users in physics and other fields of researches.

An energy change of the synchrotron is required once in a daytime to select the optimum residual range for different patients. After changing the beam energy, the dose uniformity in the irradiation field is checked. Before and after the daily treatment, energy and beam course is changed for the basic experiments.

Total of 37 weeks per year are available as machine time, other 2 weeks are for beam tuning and 13 weeks are scheduled shut down for machine maintenance *etc*. About 1,500 hr. per year was spent by the clinical trials and about 2,500 hr. of machine time is assigned to the basic experiments and beam tuning.

All devices of HIMAC are controllable through a digital computer system. Optimized set of the operation parameters are saved in a specified file and usable in the next operation. With a well established operation file, it takes only 20 or 30 min. to tune a pair of the synchrotron rings. It requires nearly the same time to fix the HEBT parameters including the tuning time for the beam switching. The injector, however, needs more than one hour, because it takes about 30 min. for an ion source to get stable.

The reproducibility of the beam performance is excellent without manual tuning of the magnetic fields. In order to minimize the field variation due to a hysteresis loop, an initializing technique is introduced before setting the magnet currents. During the initializing process, all magnets are excited with the maximum currents of the power supplies. By following the same path of the hysteresis loop, the magnetic fields well reproduces the previous values with only setting the magnet currents.

4. Beam Performance

We have two types of ion sources: a PIG and an ECR sources installed independently on high voltage decks of 60 kV max. The output beam intensities and emittance of both sources are satisfactory for the treatments[4],[5]. The beam transmission efficiencies through the low energy transport line and the RFQ are attained to be around 80% and 90%, respectively, in daily operation. An example of the output beam signal of the injector is given in Fig.1 together with rf pulses for RFQ and DTL.

The two synchrotron rings are operated independently from each other except that the magnets must be excited 180° out of phase. The dipole field changes from 0.11 T at injection energy to 1.5 T at maximum with a ramping rate of 2 T/s (max). The betatron tunes are chosen typically at 3.68 and 3.13 for horizontal and vertical directions, respectively. A typical operation pattern of the ring magnets is 200 ms for a flat base, 700 ms for rise and falling time and 400 ms for a flat top. In Fig. 2, an example of oscilloscope signals is given for a bending magnet excitation pattern (top), a bump magnet for beam extraction (2nd), beam signal in the synchrotron ring (3rd) and the extracted beam signal (bottom). In the signal of the extracted beam, very big intensity fluctuation can be observed. This fluctuation is due mainly to a current ripple of the synchrotron magnets, because no feedback system is applied to stabilize the extracted beam intensity.

High frequency components of the beam ripple are suppressed appreciably after careful tuning of the synchrotron magnet power supplies. At the flat top, voltage ripples of the power supplies of Q_F and bending magnets are kept extremely low values of less than 1×10^{-6} and 1×10^{-5}, respectively (50 Hz). A beam ripple, however, remains at high level. By reducing the sextupole fields for chromaticity correction, satisfactory beam spill is obtained as shown in Fig. 3. This fact means that the fluctuation of the bending field may affects strongly on the beam ripple through the sextupole fields.

The whole control system works very well and even a very low intensity beam of a few hundred particles per second can be stably accelerated without $\Delta\phi$ and Δr feedback loops.

In order to get a high efficiency of the treatment room usage, it is required to switch the accelerated beam from one treatment room to the other room in a very short time. The beam switching must be done

without introducing the beam into the treatment room. The reproducibility of the beam position should be better than ±2.5 mm at the isocenter. Such precise beam positioning is realized with a special sequence in the switching magnet excitation. The new technique for beam switching takes only 5 min. and will be adopted in the actual treatment in near future.

5. Future Developments

HIMAC facility is open for many researchers who are interested in the heavy ion science as well as heavy ion therapy. In many researches, HIMAC is required to accelerate heavier ions with a variety of energies and with high quality. In order to meet these demands, third ion source of 18 GHz ECR source is now under development. Ions from these three ion sources will be accelerated simultaneously with so called time sharing acceleration scheme and delivered to a medium energy experimental room, the upper synchrotron ring and the lower synchrotron ring.

A secondary beam will be available within a few years to investigate the possibility of precise check of the ion stopping position in a human body. The positron emitters, such as ^{11}C, are considered to be effective for this purpose. The beam course will be open for other scientific fields.

Further sophisticated irradiation schemes, such as a spot scanning method or a three dimensional irradiation method, are also important in improving the effectiveness of the heavy ion therapy. An irradiation treatment synchronized with human breathing is our first target to reduce the unwanted dose to the normal cells around the tumor. The treatment will be realized with a quick response of the rf-knockout beam extraction from the synchrotron ring[6].

6. Acknowledgments

The authors express their sincere gratitude to Drs. Y. Hirao and K. Kawachi for their continuous encouragement and fruitful discussions. They are also grateful to other members of AEC for their skillful assistance.

7. References

[1] Castro *et. al.*, Int. J. Rad. Oncol. Bio. & Phys., **29**, 647 (1994).
[2] K. Sato et al., Nucl. Phys. A588, 229 (1995)
[3] S. Yamada, Proc. 1995 PAC, USA, to be published.
[4] Y. Sato *et. al.*, Rev. Sci. Instrum., **63 (4)**, 2904 (1992).
[5] A. Kitagawa *et. al.*, Rev. Sci. Instrum., **65 (4)**, 1087 (1994)
[6] K. Noda et. al., EPAC94, to be published.

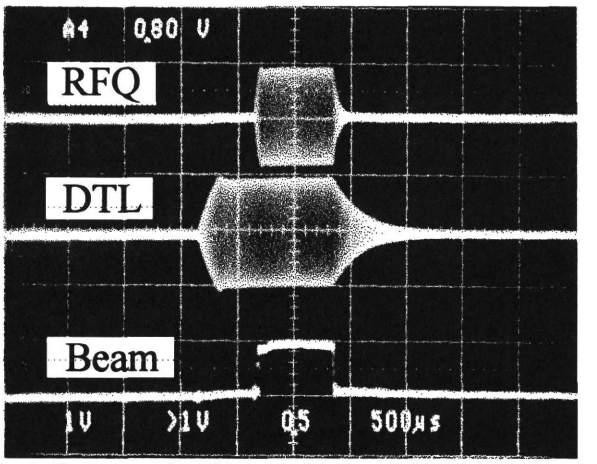

Fig.1: An example of beam signals of the injector.

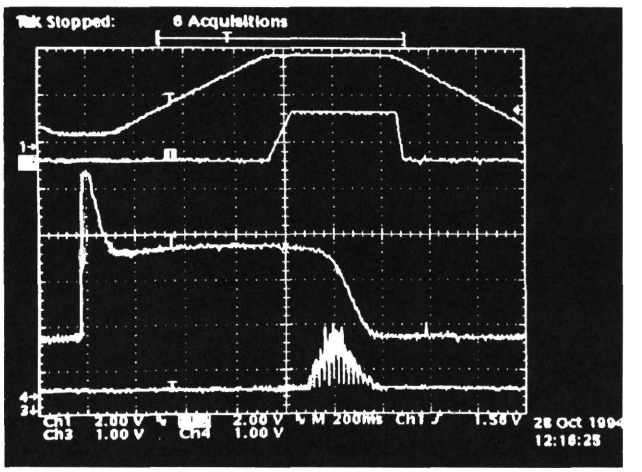

Fig.2: A typical example of beam signals in the synchrotron. See text for more details.

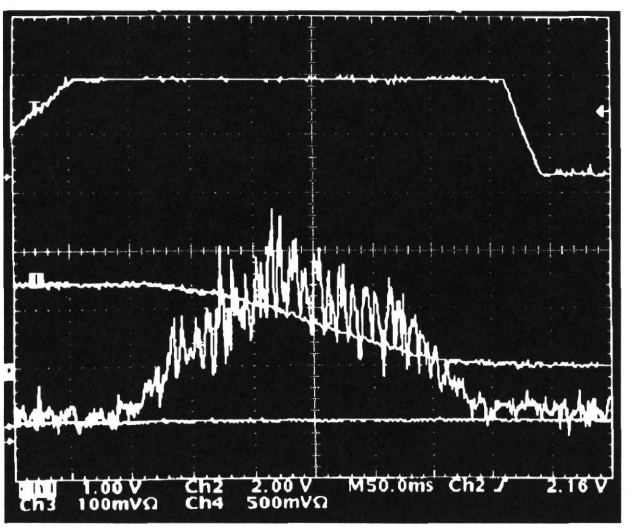
Fig.3.: An example of the beam spill from the synchrotron. See text for explanation.

DESIGN OF SOLENOIDAL MAGNETS WITH LAMINATED CORES

E.Tanaka*, S.Yamada, T.Murakami, A.Kitagawa, H.Ogawa,
T.Fukushima*, T.Kimura*, O.Morishita**, T.Sakata**, K.Sawada**

National Institute of Radiological Sciences (NIRS), 4-9-1 Anagawa, Inage-ku, Chiba 263
*Accelerator Engineering Corporation, 2-10-14 Konakadai, Inage-ku, Chiba 263
**Sumitomo Heavy Industories, Ltd., 5-2 Soubiraki, Niihama, Ehime 792

Abstract

HIMAC (Heavy Ion Medical Accelerator in Chiba), which is the first heavy-ion accelerator facility for medical use in the world, is in operation at NIRS. A project of time-sharing-operation of the injector is in progress and a solenoidal magnet with a laminated core is designed and assembled for the time-shearing-operation of the injector. Specifications and results of magnetic-field measurement are described.

Introduction

The HIMAC facility can be divided into three parts; the injector, the synchrotron with two identical rings, and the irradiation system with horizontal and vertical-beam lines. The injector comprises two kinds of ion sources (ECR and PIG), two kinds of linear accelerators (RFQ and Alvarez linac), and beam-transport systems. The linacs accelerate various ions of 8 keV/u, ranging from He to Ar, up to 6 MeV/u. A medium-energy beam line, in cooperation with two pulse-operated magnets, can supply beams to three beam lines, i.e. two synchrotron rings and a medium energy experimental room (see Fig.1), 'simultaneously', changing the beam directions from pulse to pulse.

In order to increase the versatility of the facility, the time-sharing-operation of the injector, i.e. acceleration of different kinds of ions from pulse to pulse, was studied and the project is in progress. In the present case operating parameters of all devices will be adjusted to the optimum values so that ions with values of largely different q/A can be accelerated. All the magnets and monitoring devices in the beam transport line must, therefore, be replaced by those bearing pulsed-operation. Since a solenoidal magnet of DC-operation is installed in the low-energy beam-transport line, in addition to the electro-static quadrupole lenses, a new solenoidal magnet with a laminated core is designed and assembled.

Structure of the solenoidal magnet

Specifications of the solenoidal magnet are listed in Table 1 and its dimensions and structure are displayed in Fig.2. A coil of 288 turns with a current of 350 A generates maximum magnetic field of 6.8 kGauss at the center. A water-cooled coil is made of the hollow copper conductors. A magnet core consisted of two types of segments, Core-A and Core-B (see Fig.2), both of which are made of 0.5 mm thick steel plates coated with electrical insulators. The Core-A is a pile, 25 mm thick, of octagonal plates and is fixed to the Plate-A being made of SUS304. Rectangular plates of 65 mm × 218 mm in size are piled up to form eight pieces of Core-Bs; six of them are 160 mm thick and two of them are 130 mm thick. Each one is tightened by bolts and Plate-Bs, then fastened to the plate-A. The coil is also fixed to the Plate-A with supporting rods.

All the components, cores and the coil, were bolted, and no welding method was employed. It is, therefore, free from the strain induced by the welding. End faces of the coil, which define the spacing between Plate-Bs, were carved with accuracy of $\leqq 0.2$ mm. Overall accuracy is within ± 0.5 mm by controlling torque of the bolts. Omission of the welding process can cancel out the additional cost due to longer machining and assembling processes.

Magnetic-field distribution

Measurement of magnetic-field distribution was carried out. The current source was operated in a DC mode. An example of the field distribution is shown in Fig.3 for the cases of I = 50, 100, 150, 200, 250, 300, 350 A. An effective field length was calculated to be 180 mm. Relation between the maximum magnetic field (Bmax) and the electric currents (I) is plotted in Fig.4.

The Bmax values linearly depend on the current values, so that saturation effect inside a core seems to be negligible small. The Bmax of 6.915 kGauss obtained with the current of 347 A is strong enough compared to the specification.

Laminated cores of solenoidal magnets have more complicated structure then that of ordinary dipole magnets. Our design of the new magnet can be one of the solution.

References

(1) A.Kitagawa, et al., The 5th Japan-China Joint Symposium on Accelerators for Nuclear Science and Their Applications. (1993)

Table 1
The specifications of the solenoidal magnet

Coil length	218 mm
Bore diameter	110 mm
Maximum magnetic field	6.87 kGauss
Maximum magnetomotive	1×10^5 AT
Turns	288 turns
Maximum current	347.2 A
Maximum voltage(at 20℃)	34 V
Maximum power(at 20℃,DC)	11.8 kW
Cooling water circuits	8
Pressure drop	3 kg/cm^2
Water flow	14.2 l/min
Water temperature rise	12.5 deg

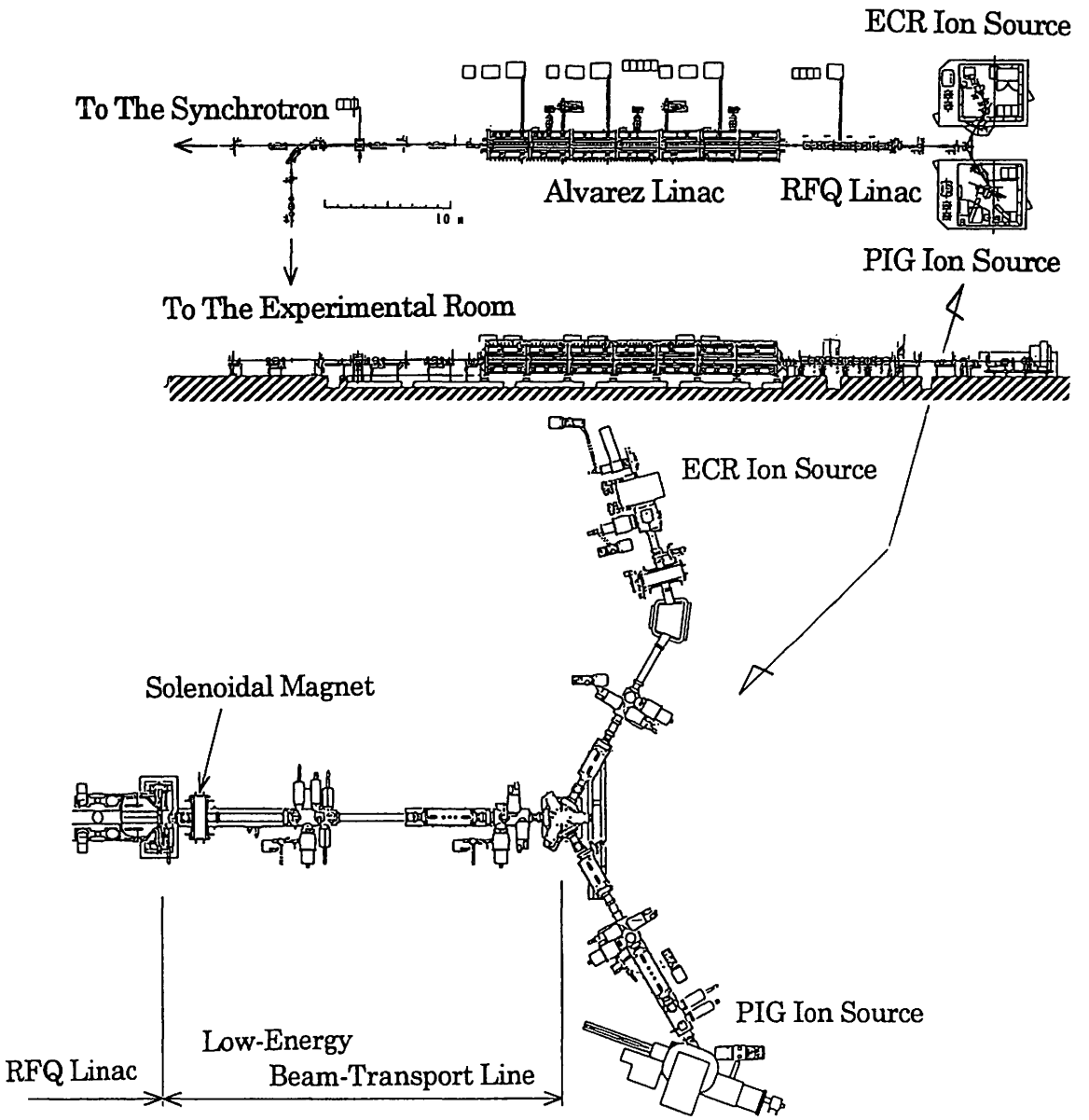

Fig.1 Layout of the injector

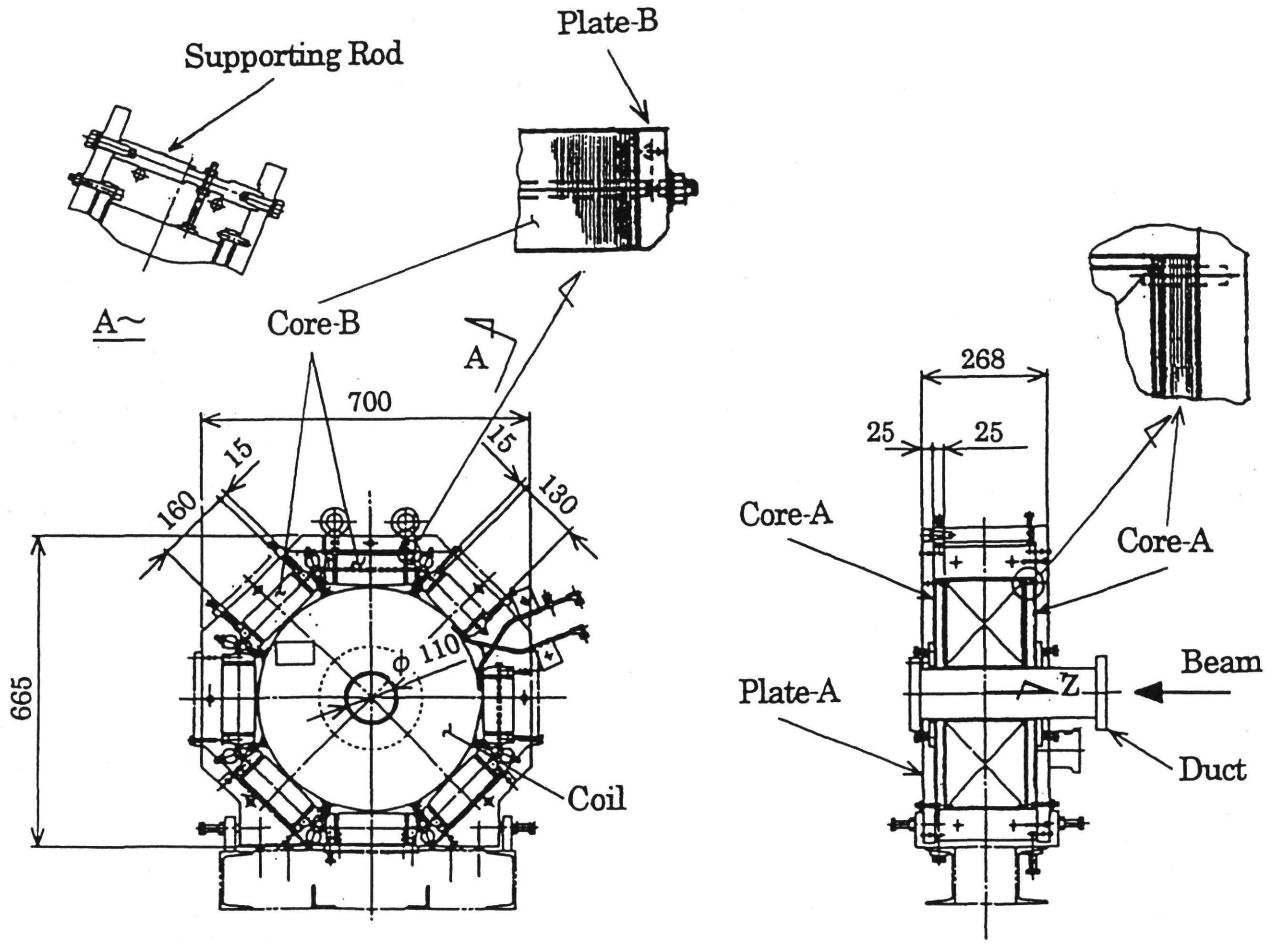

Fig.2 Structure of the solenoidal magnet

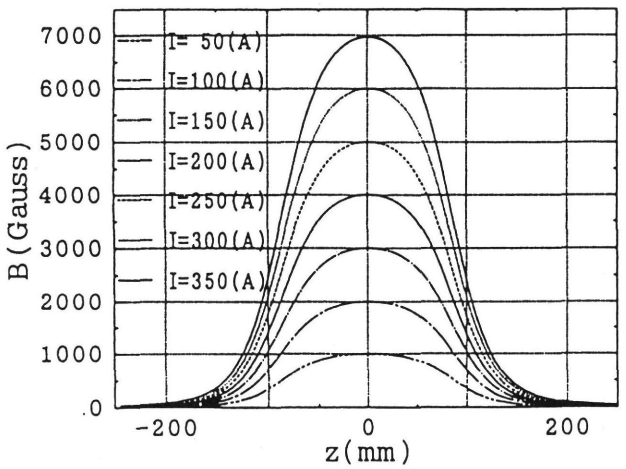

Fig.3 Magnetic field distribution

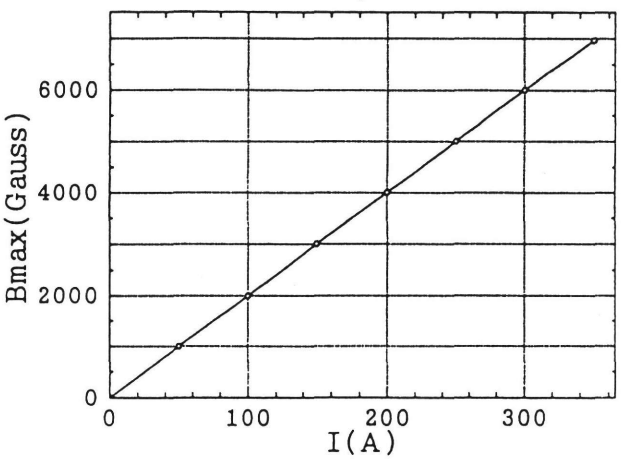

Fig.4 Relation between Bmax and I

Continuous Beam Monitoring for Charged Particle Therapy

M.Torikoshi, H.Ogawa, K.Noda, E.Takada, T.Kanai,
K.Narita*, T.Fukuzumi*, T.Kohno**

National Institute of Radiological Sciences, 4-9-1 Anagawa, Chiba 263, Japan
*Accelerator Engineering Corporation, Konakadai, Chiba 263, Japan
**Department of Energy Sciences, Tokyo Institute of Technology, 4259 Nagatsuta, Yokohama 226, Japan

Abstract

Continuous beam monitoring can ensure beam stability during beam irradiation for charged particle therapy.It can also detect the beam which is not synchronized with a patient's respiratory in case of treatment of an organ moving with respiratory. A MWPC was adapted to these purposes. It was used in air not to disturb beam. The effective thickness of the MWPC with respect to the beam is only that of wires. Therefore, scattering the beam and losing the energy of the beam in the MWPC is sufficiently small so that they do not affect charged particle therapy. The MWPC was proved to be useful by use for biology experiments.

Introduction

The Heavy Ion Medical Accelerator in Chiba (HIMAC) at National Institute of Radiological Sciences is the first heavy ion accelerator complex dedicated for charged particle therapy[1,2]. Charged particle therapy severely requires controlling dose of beam and safety assurance. In the HIMAC, the dose is measured by using two monitors, an ion chamber and a secondary electron monitor, at the same time. Occurrence of any abnormal conditions interlocks the beam irradiation through a global interlock system.

Furthermore, the continuous beam monitoring is one of strong means to ensure beam quality as follows. The first is assurance of stability of beam profile and position, because they affect beam intensity distribution at an isocenter. The second is detection of the beam which is not coincident with a patient's respiratory during the treatment of an organ moving with the respiratory. When such a beam spill is detected, the treatment is interrupted in order to make beam extraction coincident with the respiratory. Thus the continuous monitoring shall be one of the activities of quality assurance for the charged particle therapy.

Beam monitor for medical use

A multi-wire proportional chamber was in use for the continuous monitoring. The MWPC is same as that developed for beam monitors used at the high energy beam transfer lines (HEBT) of the HIMAC[3]. A picture of the MWPC is shown in Fig.1.

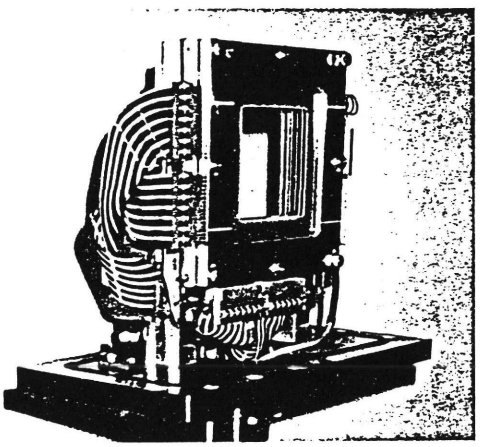

Fig.1 MWPC used in air

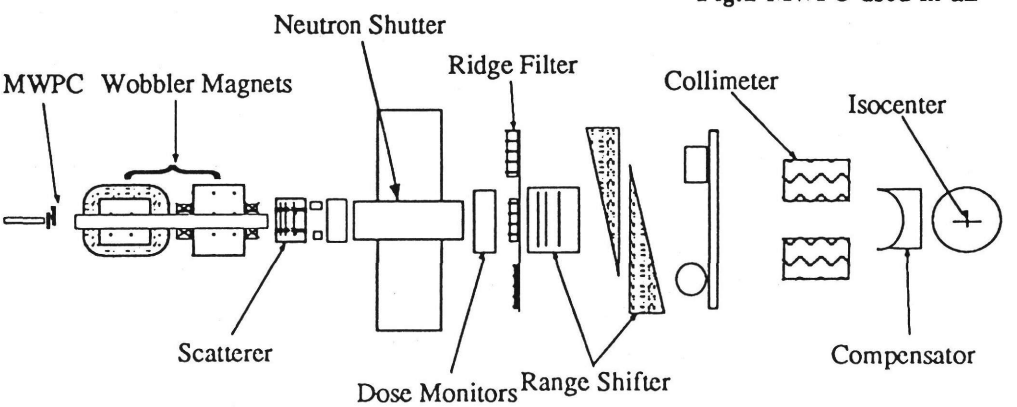

Fig.2 Configuration of the BIOLOGY beam course

Rare gases or organic gases are generally used to obtain high amplification factor of the MWPC. In these cases, thin windows are necessary on the MWPC to have gas tight structure. Our purpose is focusing to use the MWPC as a sort of non-destructive monitors, so that the MWPC should have no window on it. Eventually, air is used as the sensor gas of the MWPC. Therefore the beam passing through the MWPC has a probability to collide with only the wires. We describe the effects of the collision as an average thickness of the wires, that is approximately $8x10^{-2}g/cm^2$. This is corresponding to water equivalent thickness of only 0.8mm. This value is negligibly small in comparison with thickness of a margin on a target volume in a body.

The MWPC was installed at the end of BIOLOGY beam line as shown in Fig.2. The MWPC is located between the end of beam duct and Wobbler magnets. The beam intensity is uniformly distributed at the isocenter by a pair of Wobbler magnet and a scatterer. Each wobbler magnet sweeps sinuously the beam in horizontal or vertical direction. Combination of both motions of the beam results in rotational motion. The rotating beam is scattered by the scatterers. In this way, the beam of maximum diameter 22cm become uniform within ±5% at the isocenter. Scattering effect at the MWPC affects the uniformity. However, the effect evaluated by a calculation is only less than $1x10^{-3}$%. Eventually the MWPC can be regarded as the non-destructive monitor for the charged particle therapy.

Electronics

We used the same electronics with that used for the beam profile monitors of the HEBT[3]. Generated current on a wire of the MWPC is integrated on a capacitor in the integration circuit.

The electronics gives us good performance as follows. Typical noise level is 1 digit of full scale 2048-digit. The noise level is independent of the time width of integration. It means that leak currents in electronic elements do not contribute to the noise, or are very small. A simple estimation shows that the leak currents are supposed to be less than 0.1nA each channel. Cross talk between adjacent channels is less than -60dB. Because of the low noise level and the small cross talk, the beam profiles can be observed clearly even though the peak height of the profile is less than 0.1V.

Tests and results

In order to test the MWPC under various beam conditions, the MWPC was installed in BIOLOGY beam course as mentioned above. The BIOLOGY beam course is used for biology experiments and not therapy.

Fig.3 shows dependence of the gas amplification factor on applying voltage. It was measured at C^{6+} 290MeV/u beam. The amplification curve is normalized

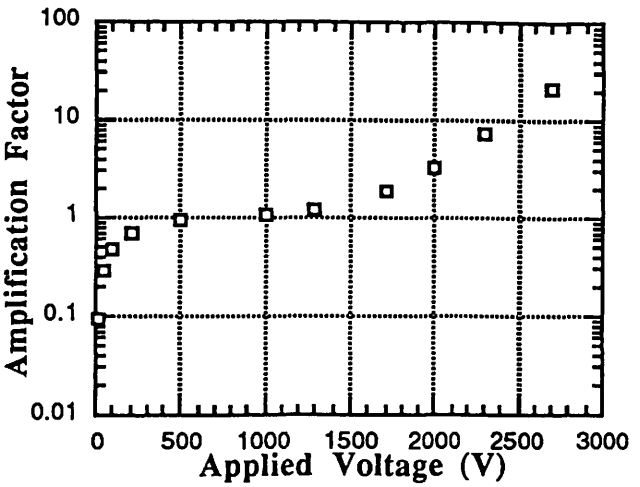

Fig.3 Dependence of amplification on applied voltage

to 1 at plateau region. Because the amplification factor should be 1 at the plateau region. The curve shows the amplification factor is about 20 at -2.7kV the maximum voltage of the MWPC. The amplification factor 20 is small compared with that of same type profiles monitors used at the HEBT. They gain more than 5,000 filling with Ar-CO_2 mixed gas[4]. Comparatively small amplification factor results from quenching effect due to oxygen. An oxygen component of air strongly quenches electron avalanche even under a considerably strong electric field. Charged particle therapy is performed using the beam intensity of $3.6\sim3.2x10^8$pps. In order to observe such a beam, the MWPC does not need to obtain a wide intensity range. This condition does not require the MWPC to have high amplification factors.

Dynamic range of this MWPC system spans from 1 to 2,000. This results from that the range of amplification factor of the MWPC is from 1 to 20, and the dynamic range of the electronics is from 0.1V to 10V as mentioned already. Then the intensity range of observable beams is estimated, for instance of C^{6+} 290MeV/u beam, to be from $3x10^6$pps to $6x10^9$pps. It is sufficiently wide to cover the intensity range necessary for charged particle therapy or related measurements except for measuring LET.

A beam profile of C^{6+} 290MeV/u beam observed by the MWPC is shown in Fig.4. The MWPC is located at downstream from the last triplet quadrupole magnets of the BIOLOGY beam course. The triplet quadrupole

magnets are forming 10mm diameter beam at the isocenter 11m downstream. Therefore, the beam has an approximate round shape as shown in the figure.

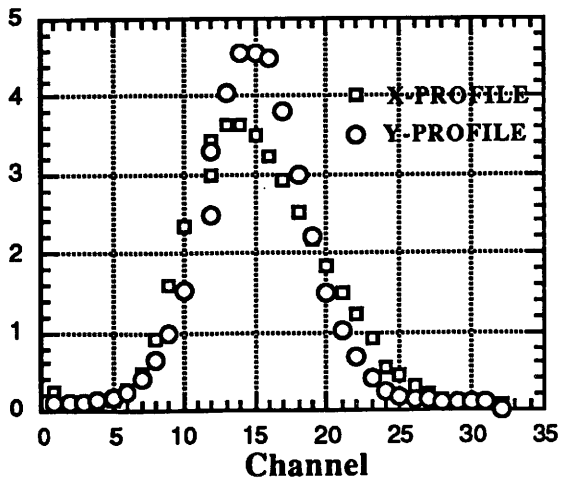

Fig.4 Beam profiles

A range of He^{2+} 150MeV/u beam in water was measured by using a water column. The measurements were carried out with and without the MWPC in the beam course. Both results are plotted in Fig.5. Circles indicate the results of the measurement with the MWPC, and squares indicate those without the MWPC. Difference between both Bragg peak positions was not detected. It means the difference is less than position resolution of the measurement.

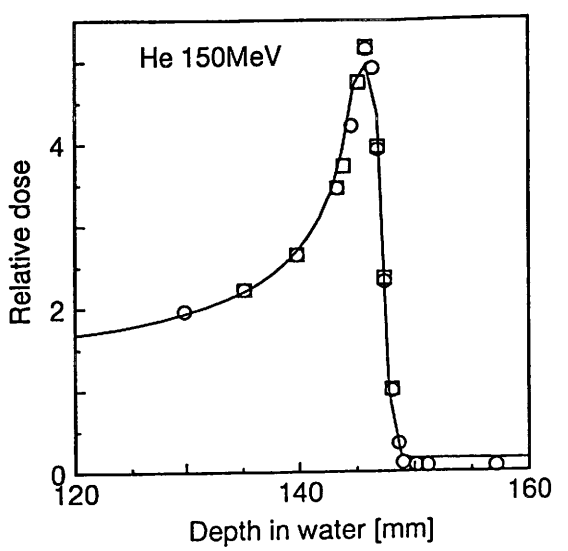

Fig.5 Dose spectra measured with and without the MWPC. Circles show results of with the MWPC.

Although an exposure of a film to the beam and scanning the density measured the beam uniformity, difference of the uniformity was undetectable as expected.

High voltage of -1kV was continuously applied to the MWPC for about 3 months. An approximate amount of total beams was 1.3×10^{14} particles. No damage due to radiation is found on the MWPC at present.

Conclusions

We summarize the results of the MWPC and these tests as follows.

(1)The MWPC worked stably in air and gained the amplification factor of about 20 at -2.7kV. The total dynamic range including that of the electronics is from 1 to about 2,000. It is sufficiently wide to monitor the beam for charged particle therapy and related measurements.

(2)Disturbance of the beam was negligibly small so that it was supposed not to affect charged particle therapy and related measurements.

We do not test the MWPC to detect the beam which is not synchronized with a patient's respiratory, because the irradiation coincident with a patient's respiratory is in a test stage at present. However, we know that the response of MWPC is sufficiently fast to interrupt the irradiation within acceptable dose ambiguity.

We can conclude the MWPC system is working as a non-destructive beam monitor with versatility to ensure the quality of treatment. A damages due to radiation of a long term, however, must be watched continuously in future.

Acknowledgment

We would like to express our gratitude to the other members of Research Center of Charged Particle Therapy of NIRS for helpful discussion. We also wish to thank the members of Accelerator Engineering Corporation for their warm support.

References

1. K.Sato et al., "Status report on HIMAC", Proc. 4th European Particle Accelerator Conf., London, 1994

2. S.Yamada, "Commissioning and performance of the HIMAC medical accelerator", Int. Conf. on High Energy Accel., Dallas, 1995, to be published

3. M.Torikoshi et al., "Development of beam profile monitor for HIMAC", The 8th Symp. on Accel. Sci. and Tech.,Saitama, 1991, pp.317-319

4. M.Torikoshi et al., "Performance of beam monitors used at a beam transport system of HIMAC", Beam Instrumentation Workshop, AIP Conf. Proc. 333,Vancouver, 1994, pp.412-418

Horizontal COD measurement and correction system in HIMAC synchrotron

M.Kanazawa, M.Sudou, A.Itano*, M.Kumada, E.Takada, K.Noda, K.Sato**, M.Katane***,J.Sagawa***, T.Miyaoka****, E.Toyoda****, and T.Yagi****

National Institute of Radiological Sciences.
4-9-1 Anagawa, Inage-ku, Chiba-shi 263, JAPAN
* Public Health & Environment Department, Hyogo Prefectural Government, Kobe 650
** Research Center for Nuclear Physics, Osaka University, Osaka 567
*** Hitachi Works, Hitachi LTD, 3-1-1, Saiwaicho, Hitachi-shi, Ibaraki 317
**** Toshiba Corporation, 1-1-6 Uchisaiwai-cho, Chiyoda-ku, Tokyo 100

Abstract

A horizontal COD measurement system has been made which has twelve electrostatic pick-up monitors beside focusing quadrupole magnets. The measured horizontal COD has maximum value of 14mm, and is corrected down to 2mm with simple way by use of twelve steering magnets which have been set at same places of the monitors.

I. Introduction

HIMAC synchrotron[1] has been designed to accelerate heavy ions from He to Ar. Injection energy is 6MeV/u and maximum energy is 800MeV/u for ions of e/m=0.5. The maximum required beam intensities for each ion species are determined to have dose rate of 5Gy/min. In the carbon case which is being used for cancer treatments now, required beam intensity is 4×10^9ppp. To obtain this value in the synchrotron, the multiturn beam injection scheme is adopted. Hence, horizontal and vertical acceptances of the ring are 260π and 26π mm mrad, respectively. Slow beam extraction with third order resonance is used, and this process requires extra horizontal space for last three turn. To determine the sizes of vacuum chambers and good field regions of magnets, additional spaces for residual COD after the correction are added. Hence the maximum apertures are ±122 and ±28mm in horizontal and vertical directions, respectively. Non uniform contraction and deformation of base concrete after final alignment deteriorate its accuracy, and increase the COD. To correct these horizontal CODs and maintain the machine acceptance large, the horizontal beam position monitor and the steering magnet systems have been constructed.

II. Electrostatic pick-up monitors

To measure the horizontal COD, electrostatic pick-up monitors with triangular right and left electrodes have been made. The electrodes that are 260mm long are made of stainless steel SUS316L. The aperture is 238 mm wide and 32mm height, which is defined with window frames to prevent the noise due to lost beam hitting. The capacitance is 110pF and its balances between the right and left electrodes in each monitors are adjusted within 2 pF with a movable ground plate (see Fig.1).

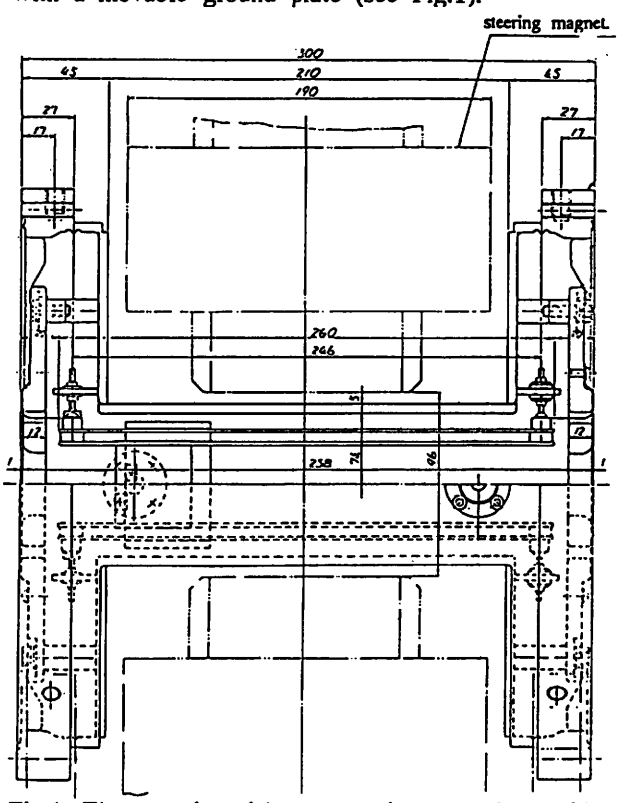

Fig.1 Electrostatic pick-up monitor together with steering magnet.

To check the output, test signal with a rod in the monitor chamber has been used. Amplitudes of

output signals from right and left electrodes (V_R and V_L) have been measured as a function of the rod position. With simple assumption the position (x) is given as follows;

$$X = (W/2)(V_R-V_L)/(V_R+V_L), \quad (1)$$

where W is electrode width. In Fig.2 the measured values of $(V_R-V_L)/(V_R+V_L)$ are plotted versus the horizontal rod position, and show linear dependence on X in the full aperture with 24% larger value of the coefficient W (294mm) than the geometrical electrode width (238mm). If there are unbalanced capacitances or setting errors of right and left electrodes, measured beam position has offset error. If this error was larger than 0.5mm, we adjusted the capacitance valance to reduce the measured position at the center.

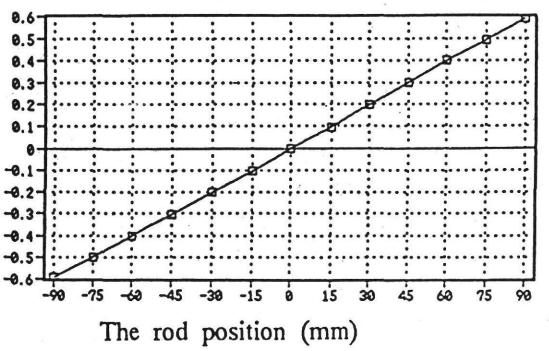

Fig.2 Output values of $(V_R-V_L)/(V_R+V_L)$ versus rod positions.

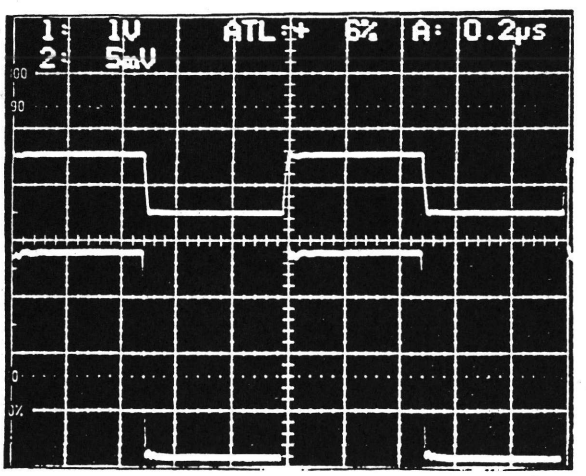

Fig.3 The upper is the input signal from signal generator and the lower signal is the measured output of the monitor electrode.

III. Monitor electronics

Monitor electronics is similar to the one[2],[3] in an acceleration system except for following points.

1) Between pick-up electrode and first FET amplifier, there is semi-rigid cable of 40cm which has resister of 100Ω in the middle. As shown in Fig.3 this attached resister permit to amplify the beam signal without distortion by the signal reflection. And this cable permit to attach the first amplifier away from the vacuum chamber and to decrease radiation damage of the FET amplifier.

2) There is only one beam signal processor for position detection, and the beam signals from twelve monitors are selected with diode switches. Isolation between input channels are better than 62dB, which value is good enough for our purpose. Switching speed is 200ns and this fast speed make it possible to measure twelve horizontal beam positions in a short time as flat base period.

At the end of signal processor a low pass filter of 1kHz is used to reduce the white noise. The measured output values are shown in Fig.4. In this monitor system, frequency range of input signal is from 1 to 8MHz, and gain range from 0 to 60 dB (range used in daily operation). With difficulty of the fine adjustment in the wide range of frequency and gain, monitor electronics have offset errors of ±2mm. Owing to the wide horizontal aperture of ±122mm, this error is acceptable.

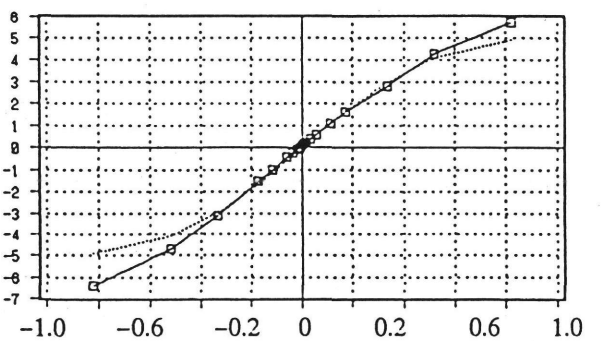

Fig.4 Output of the monitor processor versus input value of (Vr-Vl)/(Vr+Vl) with the monitor gain of 20dB and the frequency of 8MHz.

IV. Steering magnets

Twelve steering magnets have been installed at the same place as monitors to correct the horizontal COD. The magnets have been made with laminated core to make possible the pattern operation for COD

correction at flat top. Maximum field strength is determined to correct the expected CODs at the flat top field which are 16mm. The value is 800 Gauss with the magnet length of 10cm. The magnet power supplies are controlled with pattern data of 12 bits.

V. COD measurement and correction

To check the monitor, beam positions were measured for different RF capture frequencies (see Fig.5). Changing RF frequency (δf), the beam position (δx) varies as follows;

$$\delta x = \eta \gamma^2 \gamma_{tr}^2 (\gamma_{tr}^2 - \gamma^2)^{-1} \delta f/f, \quad (2)$$

where η is dispersion at the monitor, γ is the energy in units of the particle rest energy, and γ_{tr} is the value at the transition energy. In the HIMAC synchrotron γ_{tr} =3.67, η =2.5m, and γ =1.0 at injection. By use of these parameters,

$$x = 2.7 \times \delta f/f \text{ (m)}, \quad (3)$$

and this coefficient is consistent with the measured value of 2.8m.

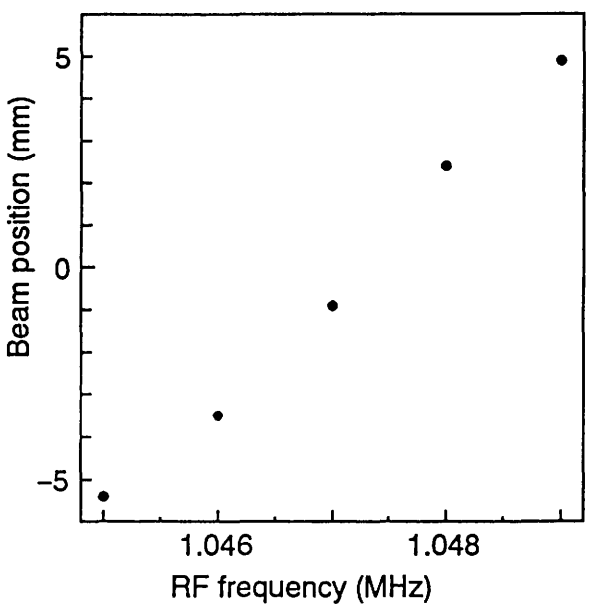

Fig.5 Measured beam positions with different RF capture frequencies.

Assuming linear lattice for COD correction, displacements of beam positions can be expressed as follows,

$$X = A\theta \quad (4)$$

where Xi is displacement of beam at the i-th position monitor, and θ i is deflection angle with i-th steering magnet. The deflection angles (θ) to correct the COD (X_{COD}) is given with the inverse matrix of A as follows;

$$\theta = A^{-1} X_{COD}. \quad (5)$$

Measuring the displacement of beam position at the monitor with excitation of one steering magnet, this matrix elements of A can be determined experimentally.

At the flat base the COD could be reduced to the value smaller than 2mm (see Fig.6) with steering magnets, whose field strengths were calculated with a equation-(5).

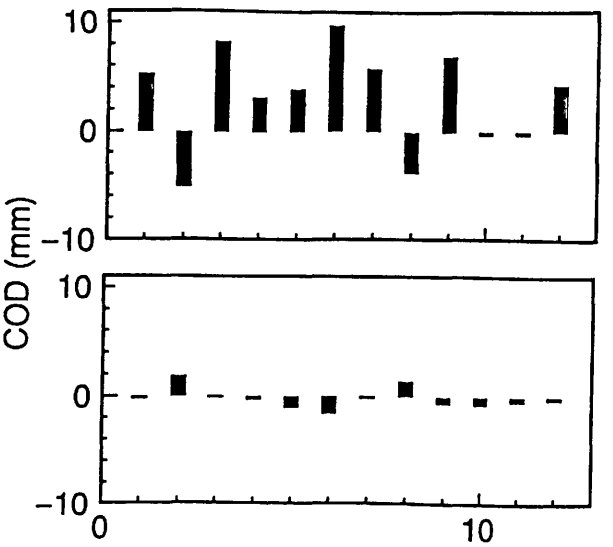

Fig.6 Measured COD before correction (Top), after correction (Bottom).

VI. Acknowledgements

The authors would like to appreciate engineers of Iwatsu electric co., LTD and Sukegawa electric co., LTD for their effort to produce the nice components in this system. they are also grateful to the operating crews of AEC for their skillful assistance.

VII. References

[1] Y.Hirao et al., "Heavy Ion Synchrotron for Medical Use," Nucl.Phys.A538,541c(1992) Y.Hirao et al.,"Heavy Ion Medical Accelerator in Chiba,"NIRS-M-89,HIMAC-001,1(1992)

[2] M.Kanazawa et al., "Beam Monitors for RF Feedback Control in HIMAC Synchrotron" Proc. of the Workshop on Advanced Beam Instrumentation, 504(1991).

[3] M.Sudou et al., "Beam Monitor of HIMAC Heavy-ion Synchrotron" Proc. of 8th Symp. on Accel. Sci. & Technol., RIKEN, Saitama,Japan, 320(1991).

Non-destructive Beam Profile Monitor at HIMAC

S. Sato, N. Araki, M. Hosaka, Y. Sano*, H. Takagi*, M. Torikoshi,
K. Noda, E. Takada, H. Ogawa, T. Honma** J. Matsui***, and T. Nagabuchi****

National Institute of Radiological Sciences, Chiba, 263, Japan
*Accelerator Engineering Corporation, Chiba, 263, Japan
**Cyclotron and Radioisotope Center, Tohoku University, Sendai, 980, Japan
***Mitubishi Electric Corporation, Wadasaki-cho, Kobe, 652, Japan
****Toshiba Corporation, Yokohama, 230, Japan

Abstract

Non-destructive profile monitors (NDPM), based on micro-channel plate (MCP), have been developed and installed in both the synchrotron ring and high-energy beam transport (HEBT) line at HIMAC. Beam test using these monitors have been carried out since April of 1995 to investigate a change of vertical beam size in synchrotron and a possibility of observing beam with high energy by one pass. In this paper the measurement system is mainly reported, and the preliminary results are also briefly presented.

1. INTRODUCTION

NDPM based on MCP has been studied and developed at many accelerator facilities [1～3], because of a powerful method for non-destructive beam diagnostics. The NDPM utilizes residual gas ionization. The ion-electron pairs created by the impact of high energy charged particles on residual gas are accelerated in a uniform electric field, and ions or electrons bombard the surface of MCP. Electrons emitted by the bombardment are multiplied in MCP when a bias voltage is supplied between both ends of MCP. The multiplied electrons in MCP. are collected to multi-anode strips or resistive anode using charge division method. One-dimensional beam profile is obtained as electric signal through a read out circuit.

NDPMs at HIMAC have been studied and installed for following purposes. (1) To investigate a change of vertical beam size of circulation beam during acceleration and extraction at synchrotron, because the measured vertical emittance of the extracted beam is not consistent with the calculated value based on the adiabatic dumping. (2) To monitor the beam profile non-destructively at HEBT during irradiation treatment of tumor. Therefore, two NDPMs have been designed, and installed to the synchrotron ring and HEBT, respectively.

The paper reports the design considerations of the NDPM and the preliminary testing results.

2. DESIGN CONSIDERATION

The NDPM consists of an accelerating electrode of ions or electrons created by a beam, a cascade-MCP with 32ch multi-anode strips and a read out circuit.

2.1 Estimation of output signal level

The expected signal amplitude obtained from a monitor was roughly estimated using the well-known Bethe-Bloch formula. The number of ion-pairs, that can be produced along the unit length of a 290MeV/n carbon beam, is first estimated. In this case, 5.7pairs/cm/Torr is obtained for the beam revolution frequency of 1.5MHz in the average vacuum pressure of $1x10^{-9}$Torr in the ring. Taking these values into account, since the gain of a cascade-MCP and the beam intensity are assumed to be 10^7 and 10^8pps, respectively, the estimated output current per channel is 44nA. In NDPM at HEBT, the output current is estimated at 2.9pA/ch under the conditions of $1x10^{-7}$Torr of the vacuum pressure and 10^7 of MCP's gain.

The estimation suggests that measurement in HEBT needs cascade-MCP to obtain large gain, and possibly worse vacuum condition, in the ring , lower gain is enough for assumed intensity. Nevertheless, cascade-MCP was adopted also for the ring to cover the request for weaker beam.

2.2 Structure of NDPM

Fig. 1 shows a photograph of the NDPM at HIMAC. The NDPM has 7 electrodes, which are arranged to realize a uniform electric-field to accelerate ions or electrons created by a beam. The field was calculated by using the code Poisson as shown in fig. 2. The maximum voltage is ±25kV. The effective area that beam can pass through is $180x75mm^2$ for measuring a vertical profile in synchrotron, and $100x100mm^2$ for a horizontal beam profile in HEBT. The electrode at the opposite end of the field cage to MCP is made of mesh, in order to use UV-rays for gain calibration of each anode. In both cases, the size of MCP is $55x8mm^2$ (Hamamasu Photonics F4772-01), and the interval between neighboring anode-electrodes is 1.7mm. The output of the MCP was

operated at 0.5kV negative to the anode strips which are at the grand level.

In the case of ring, the electric field of the NDPM may distort a closed orbit by about 8mm during the injection. In order to correct this disturbance, an additional electrode is installed at just downstream of the NDPM. This correction electrode has a similar structure to the monitor, and is fed high voltage with the inverse polarity by same power supply as the NDPM. In the case of HEBT, however, the correction electrode is not used because an orbit distortion is negligible due to one pass high energy beam.

In order to keep high vacuum in the ring, the NDPM was baked at 200℃ for 24hr before installation to the ring, and the resistor of 20MΩ to divide the high voltage to each electrode are equipped outside of the vacuum chamber to remove out-gas sources.

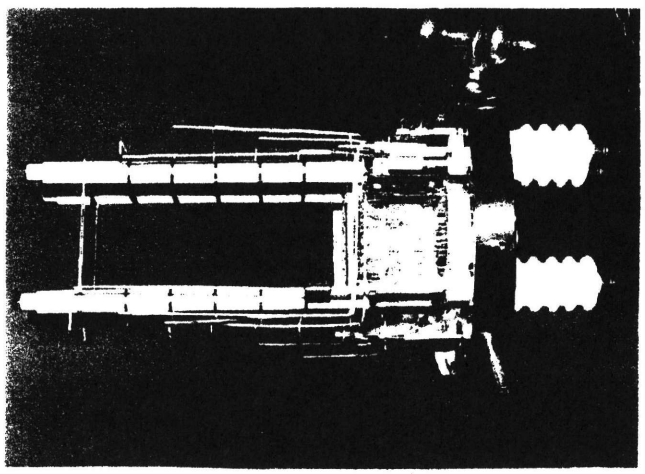

Fig. 1 Photo of the NDPM at HIMAC synchrotron.

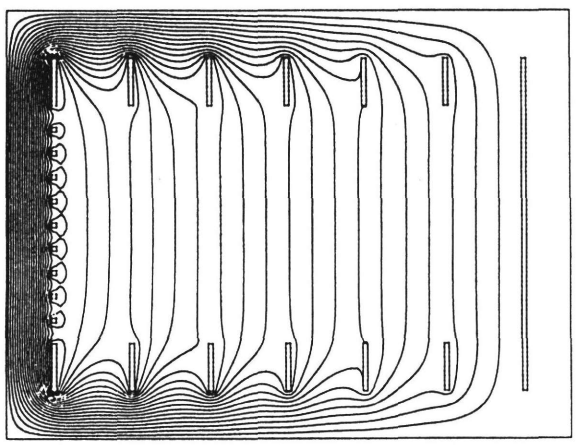

Fig.2 Equipotential line calculated by Poisson code. At the left is the mesh electrode and MCP position is at the right end.

2.3 Read-out circuit and control system

Fig. 3 shows a schematic block diagram for the read out circuit and control system. In the case of ring, the charge from the anode strip is converted to a voltage with the conversion ratio of 1V/nA, then it is digitized after a 32ch analog-multiplexer. The digitized signal is thirdly stored in a memory. The signal acquisition is repeated in this way for 1.4s at the minimum interval of 10ms. The stored data is transferred to the control computer in the central control room, and finally displayed on a CRT. The local control system is connected to the control computer through GPIB. The operation of the NDPM is normally carried out at the central control room. In the case of HEBT, generated current signal in the NDPM is integrated in the existing read out circuit with exchanging a capacitor from 10000pF to 500pF, which is used for multi-wire proportional counter type monitor[4]

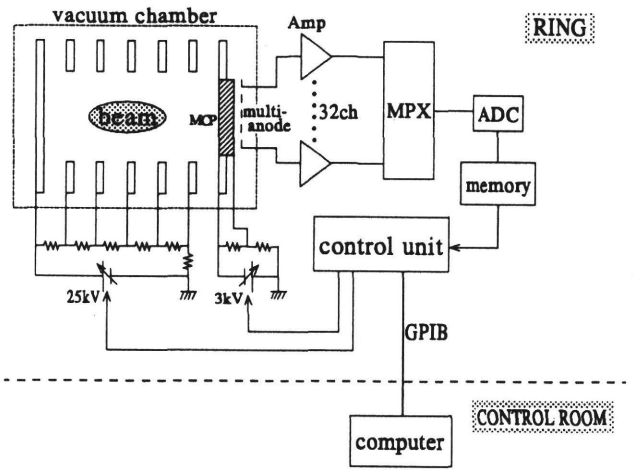

Fig. 3 Block diagram of read-out circuit and control system.

3. PRELIMINARY TEST

3.1 Calibration

UV-rays were irradiated to investigate uniformity in the gain characteristics of MCP. Results of both before beam test and after 300hr beam exposition are shown in fig. 4. As can be seen in fig. 4(a), the uniformity of gain was within ±5% at NDPM in the ring before beam test. In the case of ring, however, since the created electron intensity is somewhat high due to high revolution frequency, the gain seems to become small gradually . It is thus necessary to compensate the gain deterioration. At present, the fluctuation of the gain in each channel is measured by using UV-rays, and it is compensated in the level of software, resulting in a flat response on a CRT. In HEBT, since the created electron intensity is usually small due to one pass beam, such gain deterioration has not been observed yet.

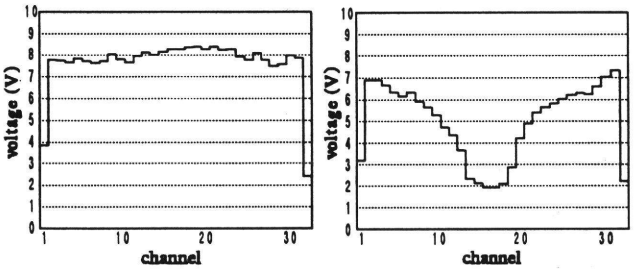

(a) (b)

Fig. 4 Gain characteristics of anode channels of NDPM in the ring. (a)before beam test. (b)after 300hr use.

3.2 Profile measurement

As shown in fig. 5, the beam profiles can be observed in both cases of ring and HEBT under the conditions summarized on Table 1. In the case of ring, signal levels were decreased as increasing a beam energy, because of reduction of energy loss.

When a correction electrode was not used in the ring, a decrease by 20～30% in the beam intensity was seen due to the kick by the accelerating electric field of the NDPM. Such a decrease was compensated by using the correction field. In HEBT, when the supplied voltage to the accelerating electrode is higher than 20kV, an increase in the noise can be found. As long as the vacuum pressure is better than 10^{-7}Torr, this noise remain very small, however the beam profile was not satisfactorily observed.

Table 1. Testing conditions.

	synchrotron	HEBT
beam	C^{6+}	Ne^{10+}
vacuum	$1x10^{-9}$Torr	$3x10^{-7}$Torr
energy	6～350MeV/u	400MeV/u
intensity	$5x10^{8}$pps	$1x10^{8}$pps
MCP gain	$5x10^{4}$	10^{7}
field voltage	～17kV	～20kV

4. SUMMARY

The NDPMs at HIMAC have been designed and tested. As a preliminary result, they measured the expected beam profile in both the cases of ring and HEBT. Both in the ring and HEBT, the measured output was consistent with the estimation. In HEBT, however, the beam profile was not satisfactorily observed when the vacuum is better than 10^{-7}Torr and the beam intensity lower than 10^{7}pps.

5. ACKNOWLEDGEMENTS

The authors would like to express their thanks to the crew of Accelerator Engineering Corporation for skilful operation of the HIMAC, and to Dr. K. Kawachi, Dr. S. Yamada and the other members of the Division of Acc. Phys. and Eng. at NIRS for their warm supports.

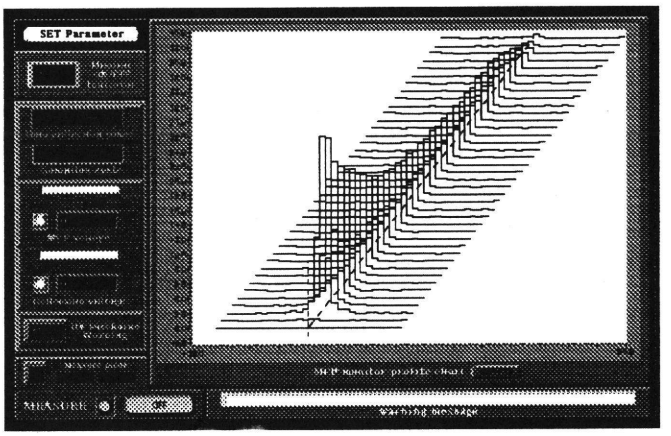

(a)

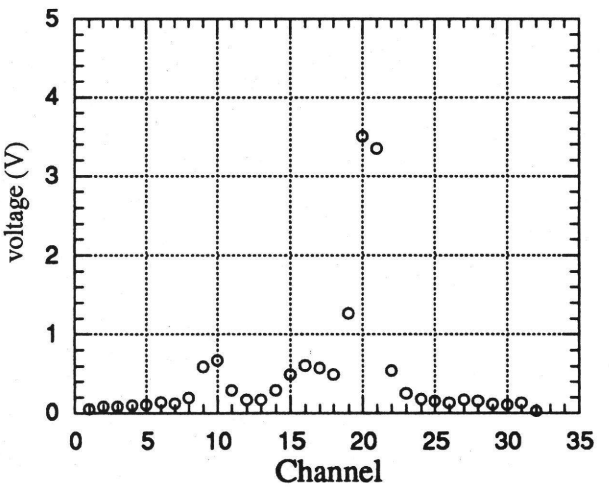

(b)

Fig. 5 Measured beam profile. (a)synchrotron.(from injection to the end of extraction, the interval of 30ms), (b)HEBT

6. REFERENCES

[1] B.Hochadel, MPI H-1990-V-19.
[2] T.Kawakubo, et al., Nucl. Instr. and Meth. A302(1991)397.
[3] T.Honma, et al., INS-T-521,p.43.
T.Tanabe, ibid., p.49.
[4] M.Torikoshi, et al., AIP Conf. Proc. 333, eds. G.H.Mackenzie, et al., p.412

Submitted to The 10th Symposium on Acclerator Science and Technology, 1995, Hitachi-naka

A BEAM SPILL CONTROL SYSTEM AT HIMAC

N. Araki, K. Noda, E. Takada, K. Sato*, A. Itano**, M. Kanazawa, M. Kumada,
Y. Yamamoto***, S. Sato, M. Torikoshi, Y. Sato, S. Yamada and H. Ogawa

Division of Acclerator Physics & Engineering, National Institute of Radiological Sciences, Chiba, Chiba 263, Japan
** Research Center for Nuclear Physics, Osaka University, Ibaraki, Osaka 567, Japan*
*** Public Health & Environment Department, Hyogo Prefectural Government, Kobe, Hyogo 650, Japan*
**** Electronics & Control System Department, Hitachi Zosen Corporation, Osaka, Osaka 554, Japan*

Abstract

A beam spill control system has been designed and installed in order to improve a spill structure of extracted beams from synchrotron at HIMAC. The system concept is to optimize a current setting pattern for correction quadrupole magnets (QDS), by utilizing an iterative control based on information of a spill structure from the beam ripple monitor.

1. Introduction

A high accuracy for the dose distribution is required in heavy ion therapy because of its sharp localization and high RBE (relative biological effectiveness). It is thus necessary to obtain a uniform dose with sharp boundary in the lateral direction, and to control precisely the total dose per patient. An irradiation system at HIMAC adopts a beam wobbling method along with a scatterer to obtain such uniformity within $\pm 2\%$ [1]. However, when a frequency of ripple in the extracted beam spill is close to the driving frequency of wobbling magnets (57Hz), the dose uniformity can be lost due to a beat phenomenon.

In a resonant slow extraction at HIMAC, a main ripple of beam spill is caused by a current ripple generated in the power supply of main focusing quadrupole magnets (QF), which is 100Hz. It is monitored with a thin scintillator at extraction beam line. A signal of harmonics synchronizing with the PLL (phase locked loop) was fed forward to the active filter of QF power supply, which was effective to reduce ripple [2]. This observation suggests a possibility of ripple reduction by quadrupole components. A beam spill control system has, therefore, been developed in order to reduce a beam ripple and to secure uniformity by shaping a spill envelope. A set of QDS, originally installed for tune-shifter, is utilized in the system. This paper reports a design consideration and preliminary experimental results concerning the beam spill control system.

2. Design Consideration

2-1. Framework

As mentioned above, basic component of ripple reduction is harmonics of power supply driving frequency. Superpositioned harmonics forms starting point of QDS output current pattern. However, there must be other sources of ripple and also fluctuation in AC line, for example, affect actual ripple output. An adjustment is necessitated for current setting to reflect these effects. It means that our system should have a function of feed forward setting and feed back from ripple signal. Iterative control of current pattern by beam signal would provide long term operability against various fluctuation conditions.

2-2. Optimization Algorithm

The important aspect of the system is an algorithm to optimize a current pattern for QDS automatically by utilizing the iterative control [3] based on information of a spill structure from the beam ripple monitor.

Assumptions on the algorithm is summarized as follows: (1) transfer function concerning the parameters of digital filter and a power supply are known; (2) the extracted beam spill is reproduced at each operation cycle of synchrotron while the beam intensity is fluctuating; (3) gain of the iterative control can be optimized in order to make the control system stable.

The optimization for the current pattern is carried out separately at low (for shaping a spill envelope) and high (for correcting a beam ripple) frequency regimes, as shown in fig.1. At a low frequency regime, an error between the spill signal after the low-pass filter and a current pattern is fed back to QDS after averaging. At high frequency regime, the spill signal after the band-pass filter with phase compensation is fed forward to QDS. Each filter is employed a FIR (finite impulse response) digital filter because of considering stable. The optimization is completed when a root mean square of the error between the spill signal and the pattern becomes smaller than a specified value. Parameters of filters at both frequency regimes as well as the feed-back and feed-forward gain are designed to be adjustable.

2-3. Structure of hardware

A beam spill controller and QDS magnet power supply have been developed to realize the system algorithm. The system structure is shown in fig.2.

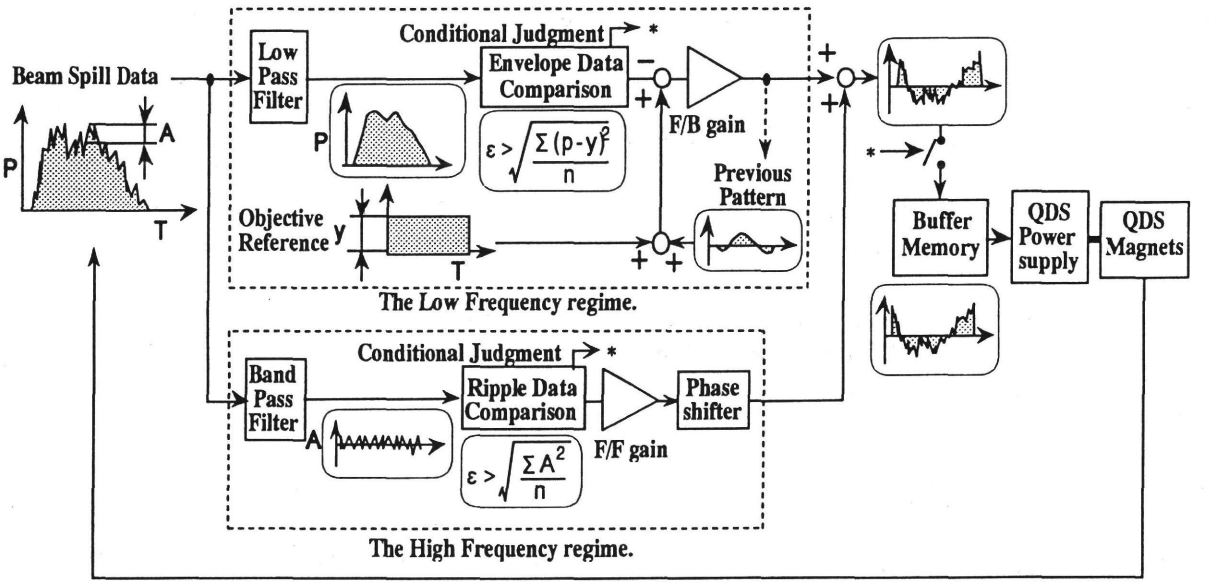

Fig. 1 Each algorithm enclosed by broken lines indicates the low and high frequency regimes.

QDS power supply is designed to have bipolar outputs, so that QF current pattern can be the same with or without the beam spill controller system. QDS power supply is operated according to the current patten that is produced based on the beam waveform.

In the control device of QDS system, VME computers are used to carry out the real-time control. VME computers consists of processors, memories and I/O's in the unit, which use a digital signal processor (DSP). CPU is MVME147S, which is used for the operating and file management, DSP is DSP8031 for filtering and other pattern control function, memory is HIMV210, A/D converter is DSP8112, D/A converter is DSP8124 and clock generator is DSP8240 for making sampling clock of 6kHz. The system realizes fast I/O handling by using a "mtt Link" bus independently. The system has been designed to be maintained by E.W.S., including file management [4]. The sampling cycle of beam waveform is 1200Hz. That of the current pattern to QDS power supply is 6kHz, which was chosen to reduce

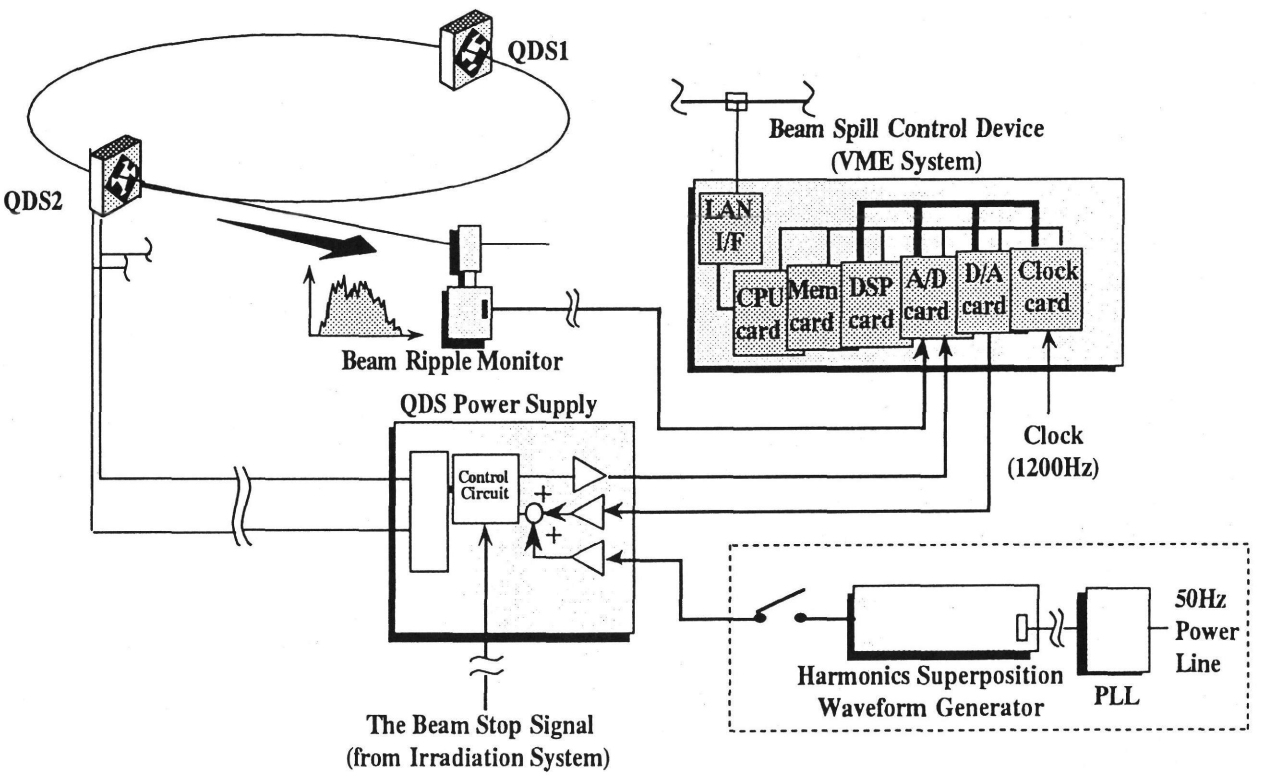

Fig. 2. Schematic diagram of spill control system and HSWG.

the peak voltage due to discrete signal.

In addition, QDS magnets and power supply are used to determine the total dose for treatment. They can directly move a horizontal tune from the resonance. When the "beam stop" signal comes from the irradiation system, forcing in QDS power supply without software handling directly realizes stopping of a beam extraction faster than few ms.

3. Experimental result and discussions

3-1. HSWG with feed forward

The experiment was carried out first by using only the "Harmonics Superposition Waveform Generator" called "Ripplebasher" [5] for the feed forward to QDS power supply. It is shown in the part enclosed by broken lines in fig. 2.

Fig.3 shows beam spills and their FFT analysis in the operation with and without HSWG, under the condition of 3×10^8pps C^{6+} beam with an energy of 350MeV/u. The amplitude and phase of HSWG were adjusted to reduce the frequency component of 100Hz at the beam ripple, respectively. The effect for ripple reduction was -14dB at 100Hz.

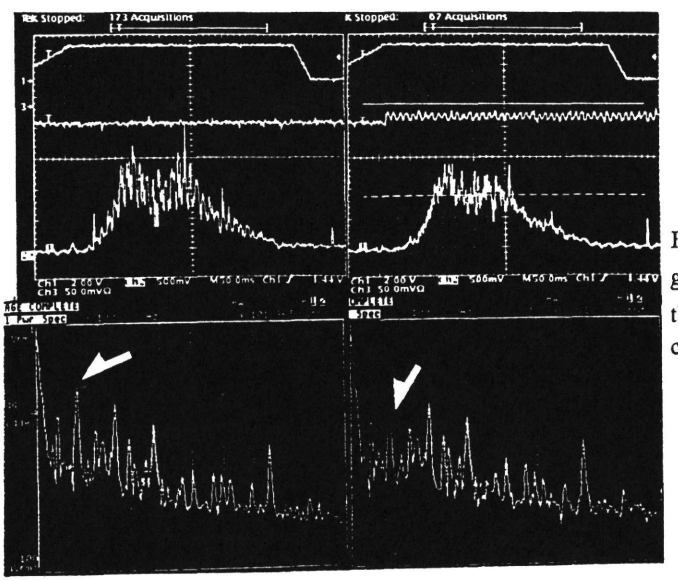

(a) (b)

Fig.3 Comparison between without (a) and with HSWG (b). beam spills and their FFT analysis are shown in the upper and lower photographs. Arrows points out a component of 100Hz.

Harmonics of 50Hz component in the case of synchronizing with the PLL was decreased by some degree compared with that in the asynchronizing case.

3-2. Computing system with VME

Encouraged by the experimental result of HSWG, the beam spill control system was tested where HSWG was removed from the system. The upper and lower limit of the band-pass filter were set to 150Hz and 100Hz. The dimensions of FIR filter are 81. The relation between the gain of the beam control system and the 100Hz component at the beam spill is shown in fig.4.

An effect in correcting the beam ripple of 100Hz has been undoubtedly recognized. However, it has not yet been satisfactory. Possible explanations are as follows: (1) the parameters of the band-pass filter seem to be inappropriate; (2) time delay due to the power supply and the load must be taken account; (3) the sampling cycle of the beam waveform seems to be too low. Next experiments will be carried out to shape the spill envelope at the low frequency.

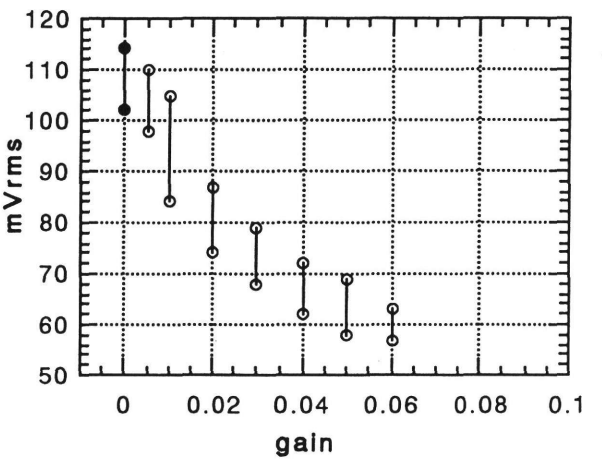

Fig. 4. Relation between the beam ripple of 100Hz and F/F gain (high frequency regime). Points at gain 0 (●) represent the ripple before the correction, while the others (○) show correction effect the system.

Acknowledgment

The authors would like to thank the crew of Acc. Eng. Corp. and to Dr. K. Kawachi and the members of the Division of Accelerator Physics and Engineering at NIRS for helpful discussions.

References.

[1] Y.Hirao et al., HIMAC report, HIMAC-001.
[2] K.Sato et al., Nucl. Phys., A558, 229(1995).
[3]T.Inoue et al., IEEEtrans, Nucl. Sci., NS-26, 3322(1979).
[4] E.Takada et al., The Hitachi Zosen tech.rev., vol.53, No.4, 1992, pp317-323.
[5] M.Kumada et al., Proc. 4th EPAC., London, 1994, pp.2338-2340.

Control system of a high energy beam transport system of HIMAC

M. Torikoshi, E. Takada, S. Yamada, H. Ogawa, K. Noda, T. Kohno*, J. Matsuura**, S.Kobayakawa**, F. Sasaki***, K. Okumura***, S. Namai***, Y. Ishikawa***

National Institute of Radiological Sciences, 4-9-1 Anagawa, Inage-ku, Chiba 263, Japan
*Tokyo Institute of Technology, 4259 Nagatsuda, Midori-ku, Yokohama 226, Japan
**Mitsubishi Electric Corporation, 325 Kamiya-cho, Kamakura, Kanagawa 247, Japan
***Accelerator Engineering Corporation, Konakadai, Inage-ku, Chiba 263, Japan

Abstract

The control system of the high energy beam transport system of HIMAC consists of a UNIX computer and a large scale interface system. Lengthy procedures, such as start-up or shutdown all the devices, can be done by only one command followed by sequential procedures in the interface system. Man-machine interface is concentrated on a console to operate easily. Total system eventually realizes the simplified operation and highly reliable performance. In this system, however, a special operation is required because of radiotherapy.

Introduction

The Heavy Ion Medical Accelerator in Chiba (HIMAC) is a complex of an injector linac cascade, two synchrotron rings, a high energy beam transport system and an irradiation system[1,2]. Each system is called sub-system, and is controllable independently. Another computer system, a supervisor system, is monitoring all the sub-systems, and also working as an interface between the sub-systems.

Beams extracted from the rings are transported to four irradiation ports of three therapy rooms, and three experiment ports through the high energy beam transport (HEBT) lines. The constituents of the HEBT system are 16 bending magnets, 69 quadrupole magnets, 39 steering magnets, their power supplies including those for the suppression coils for residual magnetic field and correction coils, 30 beam monitors, 16 vacuum units, 16 NMR sets and many other devices. The HEBT control system was required to have functions of simplified and rapid operation of the devices, software interlocks to keep patients safe and highly reliable performance because of a medical machine. The medical use also requires a special operation related with beam irradiation for treatment. In this paper, features of the system and its operation are reported.

The HEBT control system

The control system is divided into the main computer system and the interface system as shown in Fig.1. MELCOM70-MX5700II (Mitsubishi Electric Corporation) is in use as the main computer. The interface system, called MELTAC-RIO system, connects the computer and most devices of the HEBT. The computer has other interface ports of GPIB and PIO. GPIB and PIO are used for communication with NMR devices and with an interlock system, respectively. There are two sets of console as man-machine interface. These consoles are corresponding to beam lines from the upper and lower rings, respectively. Each console has 20" and 14" displays, and 3 rotary encoders. The displays are equipped with touch-panels. The computer system is connected to the supervisor system with LAN (Ethernet). Radiation dose is monitored not only at the irradiation control room but also on the consoles of the HEBT system through a LAN installed exclusively for monitoring the dose.

The interface system, MELTAC-RIO, consists of a communication unit and a group of distributed remote I/O (RIO) units. The communication unit works to arrange and manage data flow from the computer to RIO, and vice versa. Data from RIO is reformatted to be transmitted to the computer cyclically in every 200msec interval. The transmission cycle of 200msec is enough fast to monitor the system status. The computer interrupts the communication unit to send the commands (IT-message) to operate the devices. The computer can also send a file including parameters such as maximum and minimum currents, and repetition number for initialization, thus complicated procedure can be handled. The communication unit is connected to the computer with a data bus, MDWS-60.

Ten RIO units are distributed in this system as shown in Fig.1. Each unit is connected to various devices through three kinds of data bus, PIO or MELSECNET or I/O bus. The PIO connects the magnet power supplies and the relevant RIO units. DI and DO cards mounted in the units receive and transmit digital signals based on contacts or open collectors. In order to initialize the magnets, the RIO units sequentially control

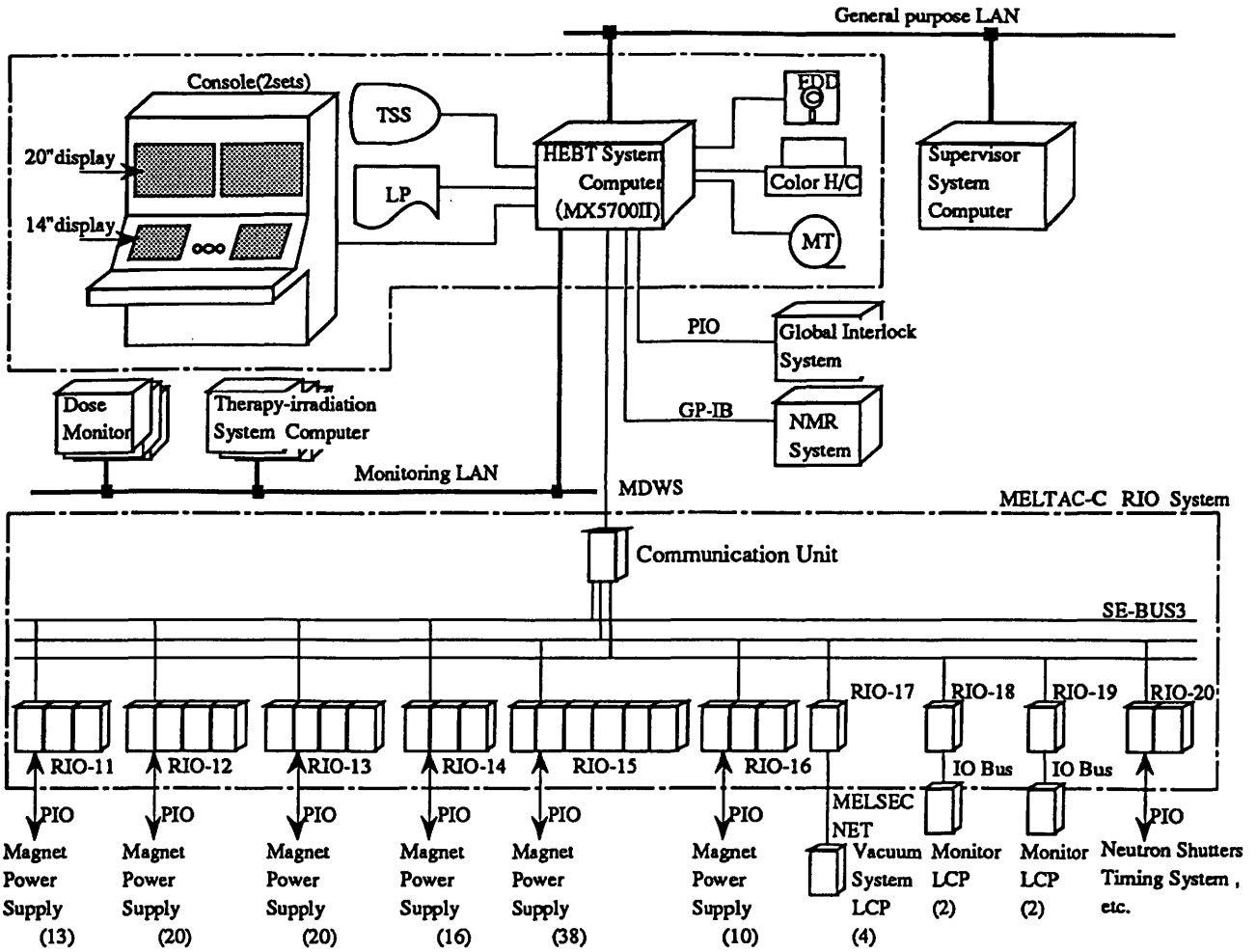

Fig.1 Schematic diagram of the HEBT control system

the power supplies according to the parameters of the initialization as mentioned above. Maximum 30 magnets can be initialized at the same time by only one command. Therefore, an arbitrary number of magnets can be initialized in short time by repeating the command. Local control panels (LCP) are distributed on the floor of the beam lines for the operation of the beam monitors and vacuum system, because it is necessary that the beam monitors and the vacuum system are locally operated in their maintenance. The devices of the vacuum system are controlled by a programmable logic controller (PLC) installed in a LCP. Four LCP's are linked in a circle, and the master LCP is connected to the RIO unit with the MELSECNET. The MELSECNET is exclusively designed for communication of the PLC. In case of the beam monitors, the DI and DO cards and buffer memories are mounted in the LCP's, not in the RIO units. Only master cards are installed in the RIO units to communicate with the LCP's through the I/O bus.

This MELTAC-RIO system deals with a large amount of data such as magnet currents, magnet status, pressure in beam ducts, beam profiles, and of operation information such as power supply ON/OFF commands, magnet initialization commands and so on. In order to realize rapid operation and monitoring, this system are cyclically processing data under a single task software using cpu's of i-80386. The cycle runs every 100msec interval in the communication unit, and 50-70msec in the RIO units. The data is transmitted between the RIO units and the communication unit cyclically through data buses, called SE-BUS3. There are three groups of the SE-BUS3, in order to reduce the amount of data of each data bus, and realize a rapid response. The data buses are summarized in Table 1, all of them being Mitsubishi

Table 1 Summary of Data Bus

Data Bus	MDWS-60	SE-BUS 3	MELSECNET	I/O BUS
Medium of Transmission	Coaxial cables	Optical fiber cables	Optical fiber cables	Optical fiber cables
Transfer Rate	15.36Mbps	2Mbps	1.25Mbps	1Mbps
Method of Transmission	Cyclic File IT-Message	Cyclic	Cyclic	Polling/ Selecting Method

Electric Corporation standard. Note that the cyclic data process and data transmission can make a maximum load of the computer independent of the amount of data, and realize stable and reliable performance.

Operation and control

Beam tunings for the horizontal or vertical course can be done independently at each console. The devices of the HEBT system are hierarchically classified with "systems", "groups" and "blocks", as in other sub-systems[3]. A block unit uniquely corresponds to a beam course. So the block classification makes it easy to switch the beam course from one to another.

The operation of starting up the whole HEBT system for new beam conditions is performed with the help of an operation parameter file. The file includes the setting values such as excitation currents of the magnets, high voltage of the beam monitors. In this operation, the magnets are initialized before excitation, and the beam monitors become ready to use by being applied suitable voltage. In about five minutes, devices are ready after the operation. Then a beam course is selected before tuning beam. Beam tuning is done for all the beam courses connected to the scheduled therapy rooms in advance of the treatments. It takes about 25 minutes for relevant beam course. Since the beam course selection is carried out by only exciting the switching magnets, the therapy room can be changed by only switching the beam course in 5-7 minutes.

Only medical operators are allowed to open the beam shutters in clinical patients irradiation. On the other hand, operators of the accelerator must handle the shutters to tune the beam. In order to prevent wrong operations, we allow opening the shutters from one console at a time, either HEBT or irradiation console. Both control systems can always close the beam shutters. Furthermore, the operators of either control system can command not to change any operation parameters of upstream sub-systems during the treatments.

Software interlocks close or prohibit from opening the beam shutters under a few conditions of the HEBT system, in order to prevent unwanted irradiation of beams. The conditions are as follows. (1)No beam course is selected. (2)Magnets and/or power supplies of the selected beam course are out of normal conditions. (3)Any gate valve of the beam course is close. (4)The computer or the supervisor system does not work. (5)The computer is disconnected from the supervisor system. Therefore the software interlocks exclude wrong operations or abnormal conditions of the HEBT system.

Summary

In the HEBT control system, a large scale interface system, and its single task processes realize simplified and rapid operation with stable performance. All the operation functions are put together on the displays equipped with touch-panels and the rotary encoders as man-machine interfaces. These features make the operators possible to operate easily and uniformly. The software interlocks are excluding wrong operations due to human errors or machine failures. Overall the HEBT control system is reliable and easy to handle, and shows good performance.

References

1. K.Sato et al., "Status report on HIMAC", Proc. 4th European Particle Accelerator Conf., London, 1994
2. S.Yamada, "Commissioning and performance of the HIMAC medical accelerator", Particle Accelerator Conf., Dallas, 1995, to be published
3. T.Kohno et al., "Control system for HIMAC injector", Proc. of the 7th Symp. on Accel. Sci. And Tech.", Osaka, 1989, pp.246-248

Present Status of HIMAC Synchrotron Control System

E. Takada, S. Sato, K. Noda, M. Kumada, M. Kanazawa, A. Itano*, N. Araki,
Research Center of Charged Particle Therapy
National Institute of Radiological Sciences
4-9-1 Anagawa, Inage-ku, Chiba-shi 263, JAPAN
and
Y. Sano, T. Togashi, H. Takahashi, M. Ogata, M. Mori, and T. Gushiken,
Accelerator Engineering Corporation
2-10-14 Konakadai, Inage-ku, Chiba-shi 263, JAPAN

Abstract

HIMAC synchrotron has been in operation since late 1993. Daily operation for irradiation of clinical trial have been executed satisfactorily. Present status of HIMAC synchrotron control system is summarized.

INTRODUCTION

As a medically dedicated accelerator, Beam must be supplied from HIMAC for treatment quite reliably. Requirements for beam energy and intensity can vary from patient to patient. Research programs which have been carried out nights and weekends also widens the variety. Under these circumstances, HIMAC synchrotrons have been operated to deliver beams for clinical trial and basic research experiments in a rather stable manner.

Of course, the individual hardware (magnets, power supplies, etc.) must be able to perform very well in order to realize stable operations. In achieving the reliable beam supply, however, synchrotron control system plays important part because it integrates the functioning of synchrotron components. Design plan and preliminary results were presented in the previous reports.[1,2] Operational experience and improvement plans are described in this report.

INITIAL TRACKING CONTROL

Synchrotron control system of HIMAC has been in operation since fall, 1993, when commissioning began. During commissioning,[3] the most crucial task of the control system was to assure tracking of BM and QF/D magnets excitation, because the scheme was to set current pattern precisely matched and to converge actual output current pattern to the preset one via repetitive, or 'self-study', control. Mechanism is an iterative application of the following procedure: The control system sets the current and voltage pattern of desired excitation to a power supply, then the system detects deviation ΔI at 1,200 Hz, or each firing pulse of thyristors, and, after averaging over several cycles, it calculates modified voltage pattern to correct current deviations. The calculation involves the presumed response characteristics of the magnet & power-supply system, and tuning was done in cut and try method prior to the beam test. Even with the pre-tuning, two aspects remained to be answered by the beam; to find an appropriate current setting pattern and to assure effective convergence of the iteration.

Although we had started from the desired values of magnetic field and the approximate expression of the current .vs. magnetic-field relation from actual field measurement, it turned out that simply applying "proportional" current setting among BM and QF/D magnets apparently suffice. Here, flat base and flat top values of currents are given and the ramping between them are adjusted in such a way that the ratio of current value to flat top value in terms of surplus from flat base value at each point is kept across BM and QF/D. This is certainly less accurate than the case from magnetic field, but more straightforward and practical in operation's viewpoint.

It was later tested with higher excitation than original 230 MeV/u or most used 290 MeV/u level, e.g., 600 and 800 MeV/u, and results were quite successful, even the field saturation effect contributes non-trivial extent at these higher excitation. Thus, semi-empirical method worked well on the first aspect of the problem: finding appropriate current

* Public Health & Environment Dept.,
Hyogo Prefectural Government.

setting pattern.

The second part was much more complicated and not yet fully understood, because the power supply itself has its own built-in voltage regulation circuitry and thus the result is a mixture of two mechanism. However empirically, convergence is obtained for each operational patterns without re-adjusting parameters for iterative "self-study" procedure. Further study is expected to exploit the feature.

STABILITY AND REPRODUCIBILITY

After the commissioning, priority of the control was given to stable and reproducible beam supply.

Clinical irradiation is scheduled weekly from Tuesday to Friday with accompanying dose measurements, and beam condition should be kept constant during the period. A patient is usually treated with 18 fractions that spans six weeks, although each fraction is normally 3-5 minutes irradiation. Since the adjustment and fixation of the patient takes typically as much as 20 minutes, beam irradiation is required to start and complete immediately after these preparatory procedure.

In this context, it is an essential performance for HIMAC that the accelerator complex keeps overall tuning for a long time and delivers beam of same conditions without re-tuning. The observation at the early stage of operation was that when the accelerator devices were kept turned-on without beam, which is stopped right after the extraction from ion source, beam was immediately delivered to the final focus when the beam stopper at ion source was opened after an overnight break.

It is also confirmed that a "file" of actually tuned operation parameters enables reproduction of the beam, thus once parameters were well-tuned, simply recalling filed parameters and setting those values secure beam delivery.

At present, carbon beams of 290, 350, and 400 MeV/u are in daily use for clinical irradiation, while other beams such as helium, neon, and silicon have been studied and provided for experimental research. For these beams, we have files of 6 MeV/u (flat base level), 100, 230, 290, 350, 400, 600, and 800 MeV/u for charge-to-mass ratio $\varepsilon = 0.5$, with basically well-adjusted parameters. Essentially, no fine tuning is necessary for different ion species, as far as $\varepsilon = 0.5$. For argon and other ions with $\varepsilon < 0.5$, one or two energy points have been studied and filed. New energy point can be developed from the existing files using the above mentioned procedure, which takes several hours.

Another evidence for stability is the fact that rf acceleration without beam feedback signal is routinely realized for a wide range of intensity; 5×10^2 to 1×10^{10} ppp.[3] In all, this means that the stability and reproducibility of the synchrotron was good enough to meet the requirement of medical application as well as research usage.

SEQUENCE AND FAULT HANDLING

One of the most practiced operation at HIMAC synchrotron is, as seen from the above, setting all devices to a reference value obtained from the file. This procedure can be done with a single set of touch operation. In the early stage of commissioning to routine operation, it sometimes got stranded and the software system of synchrotron hung-up. This was primarily caused by inappropriate handling of the sequence in the device control computers. Although corrective measures were taken, it was realized that momentary load can be larger than expected for some of the device controllers. Therefore, possible upgrade is under consideration for performance improvement.

It is important to locate fault condition that occurred during beam delivery, and to identify the cause quickly. Present control system provides error message with presumed items for each device. Recent recurrent troubles of device level include;

- decreased water-flow at magnet,
- thermo-control error at power supply, and
- rf cavity voltage over.

These were caused by defective hardware, and presumably terminated with correction on the problematic part of the hardware. On the other hand, system problem such as communication trouble happens, although sporadically. It does not seem to be a traffic congestion, but incompatible implementation of the communication protocol that is responsible, although it remains to be identified. Meanwhile, re-setting relevant computer of device control level can be postponed, since each device is set to keep operating as is when link between the controller and higher level computer is lost.

DEVICE CONTROLLERS

VME systems with MVME-147S CPU and FDI/FDO modules function for current pattern

control of synchrotron magnets and for event timing generator rather reliably. They are operated with PDOS real-time OS. Additional work station for file management serves also for development and trouble-shooting tool.

In RF/BT system, peak load seems somewhat critical, but routine operation is performed without troubles after system tuning. The rf T-clock frequency was elevated to 50 kHz for smoother transition from B-clock region and thus for smaller beam losses. While it helped, present scheme of memory module operation limits flat top time shorter than needed for 0.3 Hz synchrotron operation, thus it returned to original 10 kHz clock.

MAN-MACHINE INTERFACE

For man-machine interfacing, four VS3100 VAX Stations are used for displaying system status, beam monitor results, current setting patterns, etc. It was found that with original 16 MB memory resource/station is inadequate to respond with operator's request. Therefore, it was enhanced to 32 MB per station and now works basically fine.

Two stations are allocated for two rings each, and interface with operator by accepting touch-panel input or equivalent mouse operation. Among the panels they provide, Pattern Editing, COD, & Tune are the special feature of the synchrotron control, while the others are basically common with other sub-systems, i.e., Linac and HEBT. Those are File List, Device Status, Fault/Not_Ready List, Alarm Message List, Trend Monitors, Vacuum System, System Layout, Profile, and Slit & FCN panels.

MAIN CONTROL

The main control, CS, is VAX4000/300 with 64 MB memory, and is managing all the sequence operations and periodic data taking, as well as individual device control. It has communication with "SV", supervisory node of control system of HIMAC accelerator as a whole. Table 1 shows the processes that are running for these tasks. It is now under performance analysis to improve system throughput further.

IMPROVEMENT PLANS

In addition to what are mentioned above, a few items are considered for improving operationability and control system performance. One of the important change is "stream-lining" of pattern setting sequence, for both with and without synchrotron repetition cycle time change. Another is realization of synchronized switching of magnet and rf patterns. These improvements will enable faster and more independent change of synchrotron operational parameters such as energy, repetition cycle, etc.

Modification to facilitate new functions, e.g., respiration triggered beam control, is in progress, too.

Table 1. Processes at CS (VAX4000/300)

Name	Function
SSMP	System Self Management
MDMP	Master Display Management
FMMP	File and Memory Management
FLSP	File Load & Save
IDCP	Independent Device Control
MDCP	Monitor Display and Control
DOCP	Device Operation Control
SOCP	Sequential Operation Control
TSCP	Timed Sequence Control
RECP	Rotary Encoder Control
TCCP	TCP/IP Communication Control
SVCP	'SV' Communication Control
AEHP	Alarm and Event Handling

ACKNOWLEDGMENT

The authors would like to thank Messrs. K. Moriyama and Y. Kurei of Omika Works, Hitachi Ltd., H. Yasuda of DEC Japan, N. Tsuzuki and M. Tomizawa of Fuchu Works, Toshiba corporation, and E. Hishitani, T. Matsumoto, and K. Takahashi of Hitachi Zosen Corp. for continuous support and help.

The authors are grateful to Prof. K. Sato of RCNP, Osaka Univ., Drs. K. Kawachi and S. Yamada and members of Research Center of Charged Particle Therapy, NIRS, for discussion and encouragement. Their gratitude also goes to Messrs. K. Ueda, Y. Sato, T. Aoki, and members of AEC.

REFERENCES

1. E. Takada et al., Proc. 9th Symp. Acc. Sci. & Tech. (Tsukuba, 1993), p.73.
2. E. Takada et al., Nucl. Instr. & Meth. A352, 40 (1994).
3. K. Sato et al., Nucl. Phys. A588, 229 (1995).

Development of Dynamic Pattern I/O Modules for Advanced Accelerator Operation

E.Takada, N.Araki, A.Itano* , M.Kanazawa, M.Kumada, K.Noda, S.Sato, E.Hishitani **, S.Arai** and H.Nakagawa**

Accelerator Physics & Engineering Division, National Institute of Radiological Sciences, Chiba 263, Japan

* *Public Health & Environment Department, Hyogo Prefectural Government, Kobe 650, Japan*

** *Electronic & Control Systems Department, Hitachi Zosen Corporation, Osaka 554, Japan*

Abstract

Dynamic control of beam parameters (energy, C.O.D. etc.) is essential for advanced utilization of synchrotron beam. DPI/DPO modules are now under development to switch among various excitation patterns of main magnets and rf system while the synchrotron is operating.

DPI/DPO are VMEbus modules which provide maximum 20-bit parallel input/output port with independent 16-bit control signal port, where up to about 125kHz external clock is applicable. Dynamic switching of output pattern and other intelligent functions are performed by two RISC microprocessors, one for control and the other for calculation.

1. INTRODUCTION

Operation of synchrotron magnets are characterized by repetitive pattern which consists of injection, acceleration, extraction, deceleration and reset of beam. In order to accelerate the beam without losses, each field of lattice magnets, BM and QF/QD, should be excited in a matched strength. This is called as "tracking". Power supplies of lattice magnets, accordingly, should be precisely controlled in synchronization with the 1,200Hz trigger timing pulse of 24 phase thyrister converter for forcing power source.

HIMAC has already made use of FDI/FDO modules which were developed for this purpose [1]. Present control system of magnet power supplies works well, including event triggers that are generated from another FDO module for injection etc. However, an advancement in heavy ion therapy requires more flexible and dynamic control of synchrotron operation, as the beam delivery with pulse-to-pulse energy shift is envisaged for cancer treatment irradiation of three-dimensional scanning for HIMAC and Particle Therapy Project in Hyogo prefecture [2].

An rf system should also be operated in coordination with main magnet excitation pattern, but the clock system differs from that of main magnet power supply. T clock of about 50kHz and B clock of max. 120kHz are used for rf control. Further, B clock is of bi-directional operation to stand with fluctuation of magnetic field for both acceleration and deceleration of beam. Although the dual memory mechanism is utilized and the digital control system operates successfully [3], dynamic pattern switching is not fully realized.

Dynamic switching of these patterns (both magnets and rf) is demanded in various aspects of beam operations. For example, it is required to switch an arbitrary combination of magnets simultaneously during beam tuning or to use a set of excitation patterns as mentioned above. Usage is also expected to measure beam parameters, chromaticity *e.g.*, to initialize magnets, and to achieve digital feedback control (Iterative control or Self-study control).

Thus a dynamic pattern switch/selection is inevitable in advanced synchrotron control, which is now possible with the help of recent high-performance processors. In order to select various excitation patterns of main magnets and rf system dynamically, DPI/DPO modules are now under development. This paper describes DPI/DPO modules, with emphasis on the hardware aspect of DPO, which is developed prior to DPI.

2. FEATURES OF THE DPO

A lot of high performance RISC microprocessors for embedded system has flourished in a wide range of electronic appliances. After our investigation of abilities to handle many external interrupts and to control timer/counter substantially, we have made a choice of Hitachi Super-H (SH) series CPU which uses a 32-bit RISC core optimized for high speed and low power consumption. Another advantage of SH-1 CPU is several on-chip peripherals to eliminate many additional devices.

For a dynamic selection of a required excitation pattern from several tens to hundreds of patterns, it is necessary to discriminate many commands and to prepare enough amount of memory to store all relevant data. For this purpose 12-bit external control signal and 16MB memory are employed.

VSBbus is the subsystem standard of VMEbus.

It is provided to form a digital feed-back loop by interconnection between DPO and DPI, which is expected to correct C.O.D., for example, in real-time. Iterative control of magnet power supplies [4] will be also benefited by the DPI-DPO direct connection.

Table 1 shows the outline specification of DPO. And the block diagram is shown in Fig.1.

2-1. CPU and Memory

Multiple CPU system is provided for this module. SH-1 CPU serves to control communications with VMEbus, VSBbus and all input & output ports. SH-1 also manages SH-2 CPU which is provided for dedicated calculation. To avoid bus contentions of multiple CPU system, separate local bus is provided for each CPUs.

16MB DRAM will be used in 3 byte-word format pattern memory to cover system requirement of rf and BM operation. User supplied programs can be loaded into the DRAM of SH-1 or the dedicated SRAM of SH-2 and executed from local CPU, respectively.

Each CPU responds to commands and environment parameters placed in each 32kB dual ported SRAM which serves the accesses from the VMEbus or the local bus through the arbitration logic which intervenes synchronously with one for another when simultaneous accesses occur.

SH-2 is provided on the mezzanine board to be changeable to SH-3 CPU in future.

Input/output ports are also provided on the other mezzanine board in order to change RS485 to TTL or other interfaces.

2-2. External clock

4 bits are provided for external clocks.

- Pattern start signal (Master Clock or Rf Capture)
  It corresponds to repetitive cycle of synchrotron operation, typically ~1Hz.
- Base clock (1,200Hz or 50kHz)
  1,200Hz is fundamental clock distributed from PLL.
- Incremental B clock for rf (B+ clock)
- Decremental B clock for rf (B- clock)
  Maximum speed of B clock is presumed to be 120kHz in order to cover the BM excitation rate of 2.4T/sec at 0.2G/pulse clock.

2-3. External control signals

12-bit signal is decoded and recognized as following various events. These events are executed after next Master Clock except for Change signals that are executed immediately.

- Start & Stop
  Command to start or stop pattern output/input to devices altogether.
- Pause & Rerun
  Command to break temporarily or rerun pattern output for measurement of beam life etc.
- Selection of pattern
  Command to select any excitation pattern. Decoding method is effective to expand the range of selection, although a surplus strobe signal is necessary. It is capable to select not only any single excitation pattern but also a set of patterns and to operate partly any grouped magnets by means of masking bit, of which feature is applied to Start or Stop event when the initialization of a part of magnets is required.
- Change signal from T clock to B clock
- Change signal from B clock to T clock

2-4. Looked-Up Table

LUT is a memory to convert any data placed on the address line to another data immediately. This feature is useful to convert an accounted value of B clock to the rf frequency which is not always linear. 80k steps of table is required when BM is excited up to 1.6T at B clock of 0.2G. Then dual 80k x 20-bit memory is provided, of which one serves to make data output and the other receives next data simultaneously.

2-5. Software functions of DPO

1) SH-1 CPU for control
   - Communication with Host CPU of IOC on VMEbus
   - Communication with SH-2 CPU for calculation
   - Execution of event signal
   - VMEbus and VSBbus control
   - Initialization and placing data on LUT
   - Smoothing control of pattern
   - Data output synchronized with external clock
2) SH-2 CPU for calculation
   - Communication with SH-1 CPU for control
   - Calculation of feed-back control or data filtering
   - Smoothing calculation of pattern

3. CURRENT STATUS AND DISCUSSION

DPO with basic firmware will be prepared for performance test by the end of this year. DPO will also provide a function of timing pattern generator which produces dynamically various event control timings. System considerations, such as pattern data-base construction and management, division of tasks among host computer and DPI/DPO, are necessary to specify further details and to establish the best way of usage.

High-speed digital feed-back control with high

accuracy is attractive to challenge many technical matters of instabilities in various synchrotron operation. We expect that the combination of DPI/DPO will be useful to reduce beam ripple or to stabilize beam position by means of high-speed data acquisition and processing.

ACKNOWLEDGEMENTS

We would like to appreciate those who developed the present control system of HIMAC and enlightened us with profound understandings and discussions; Especially, Mr. N.Tsuzuki of Fuchu Works, Toshiba Corp. (rf control), Mr. S.Sakamoto of MTT Instr. Inc. (FDI/FDO system), Mr. T.Nakayama of Hitachi Inf. & Cont. Systems Inc. (magnet p/s system) and Prof. K.Sato of Osaka University are acknowledged with sincere gratitude.

We would like to thank Dr. K.Kawachi, Dr. S.Yamada and members of Accelerator Physics & Engineering Division of NIRS for discussions.

REFERENCES

[1] E.Takada et al., Proc. 9th Symp. Acc. Sci. Tech., KEK, Japan, November 1993, pp.73-75.
[2] A.Itano et al., in these proceedings.
[3] E.Takada et al., Proc. HEACC'92, Hamburg, Germany, July 1992, pp.763-765.
[4] E.Takada, T.Nakayama, E.Hishitani, HITACHI ZOSEN TECHNICAL REVIEW 53 (text in Japanese), December 1992 pp.317-323.

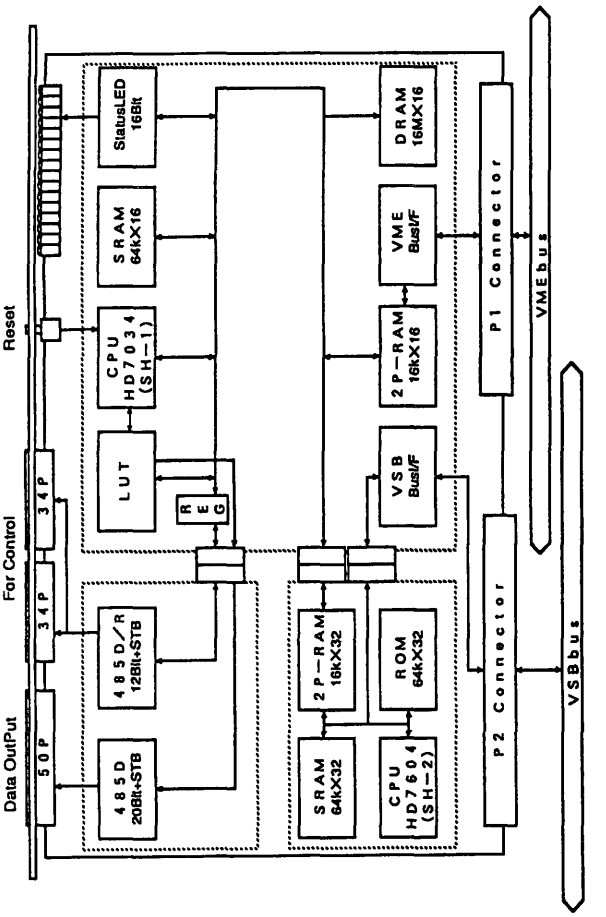

Fig.1 Block Diagram of DPO

TABLE 1 Outline Specification of DPO

	Main Board	Mezzanine Board for calculation	Mezzanine Board for I/O adaptation
CPU	SH7034(SH-1) • 4kB On-chip RAM • 64kB On-chip ROM • Hardware multiplier • 9ch. Ext. interrupt handler • 4ch. DMA controller • 5ch. Timer/Counter • 16bit Timing pattern gen. • Watch-dog timer • 2ch. Serial comm. port • Universal I/O ports	SH7604(SH-2) • 4kB cache memory • Hardware multiplier • Hardware divider • 15ch. Ext. interrupt handler • 2ch. DMA controller • 16bit Counter • Watch-dog timer • 1ch. Serial comm. port	Two 16bit bi-directional control signal port with strobe (Opto-isolated RS485 interface) 20bit+Strobe output port (Opto-isolated RS485 interface)
Clock	20MHz (16MIPS)	28.7MHz (25MIPS)	
SRAM	128kB with zero wait state	256kB with zero wait state	
DRAM	16MB with zero wait state	-	
Dual-ported SRAM	32kB with one clock wait state	64kB with one clock wait state	
LUT SRAM	384kB with 20bit U/D counter	-	
Front panel functions	16bit Status LED Reset switch	-	
Bus spec.	VMEbus IEC821 compatible slave interface (A24,D16) VSBbus IEC821 compatible master/slave interface		
Operating condition	Power source: 5V±5%, typ. 3A 5V±10%, typ.1.5A (I/O isolation p/s supplied from front connector) Temperature : 0℃~50℃ Humidity : 30%~90% (Non-condensing)		

Recent Improvement of Ripple Performance in HIMAC Synchrotron Power Supply

M. Kumada,K.Noda, E.Takada, M.Kanazawa, N.Araki, S. Sato, A. Itano[1],
H.Kubo[2], T. Aoki[3],S. Matsumoto[4], K.Sato[5]
National Institute of Radiological Sciences
4-9-1 Anagawa, Inage, Chiba, Japan
(e-mail) kumada@nirs.go.jp,

ABSTRACT

Ripples in the HIMAC synchrotron power supply and the admittance of the load were measured and confirmed to be small as 3 ppm for the Quadrupole Power Supply right after the commissioning. Further continued improvement was focussed on the 50 Hz and 100 Hz ripples which were major component deteriorating the spill. By re-tuning the power supply, we could reduce the ripple to a level of 0.3 ppm[1]. The study of the relation of the ripple and the beam spill revealed that the fluctuation of the beam spill is affected by the ripple in Bending magnet power supply in addition to that of the Quadrupole. After finding this fact, the beam spill became more uniform in routine operation by re-adjusting the Sextupole and Quadrupole strength. Encouraged by this performance, the Bending magnet power supply is upgraded by adding the active filter and the new DCCT. With this improvement the ripple became at a level of 0.2 ppm and the beam spill was improved.

I. INTRODUCTION

In a synchrotron the current of the magnet string has a trapezoidal form. Because of the resonant beam extraction, the ripple content should be a few ppm or less at the flat top. The basic ripple frequency f_b =1200 Hz of the power supply is given by the frequency of the power source(f_0 =50Hz) multiplied by the number of thyristors(24). The Fourier analysis of the ripple voltage also gives multiples of f_b. Another ripple with the frequency of $2nf_0$ is caused by imperfections of the local transformers and by variations in the triggering of the thyristors. Furthermore oscillatory spike voltages are induced across each thyristor. The spikes can also contribute ripple at frequencies as low as 100 Hz. Other problem associated with them is the production of noise spikes in equipment located in the neighborhood. In spite of various efforts, the reduction of spikes and ripples has been unsatisfactory for the requirement of the tolerance of the third order resonant extraction. To fulfill the requirement for beam extraction, in most of the accelerator in operation, additional mean such as spill feedback controller must be applied.

In the HIMAC synchrotron power supply, a new approach is taken.

II. HIMAC approach

We started from the proposition that the load of the synchrotron power supply is a cascaded string of the magnet inductance, its resistance and the capacitance between the excitation coil and the iron yoke. Typical magnitude of the capacitance of a Quadrupole magnet of a standard size is estimated to be a few nF. The iron yokes are assumed at a ground potential. At the HIMAC the yokes are connected by the earth line. The schematic diagram is depicted in Fig.1.

This model circuit is a six terminal circuit that has parallel and series resonance. Due to

---

[1] Hyogo Prefectural Governernment
[2] Hitachi Ltd.
[3] AEC, Accelerator Engineering Corporation
[4] Dokkyo University, School of Medicine
[5] RCNP, Osaka University

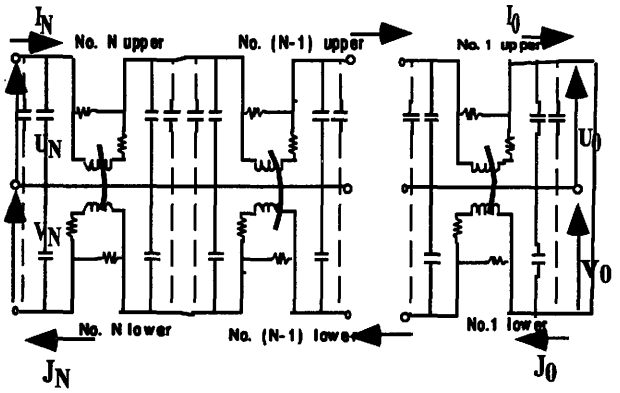

Fig. 1 An equivalent circuit of the HIMAC magnet string.

a presence of the capacitance to the ground, the incoming current I to the load and the outgoing current J from the load may not be identical as contrast to the ordinary model of without the capacitance to the ground. The difference current I-J flows back to the neutral point of the thyristor bank. The potential at the neutral point develops and is known as a common mode voltage. In the case of the grounded neutral as in the HIMAC this potential is small. In order to estimate the magnitude of the ripple current we need to know the resonance frequencies and the admittance. If the spike frequency or the ripple frequency overlap the resonance of the magnet string, the ripple current is enhanced. To avoid the overlap, the knowledge on frequency characteristic of the load is required. No previous analysis was done in the past. Computer simulation is time consuming. By applying eigenvalue technique, we found that six terminal circuit can be reduced to two set of orthogonal four terminal circuit. We found as a special case decomposition into the normal mode and the common mode is possible. The normal mode voltage and current is defined as U+V and I+J and the common mode voltage and current is defined as U-V and I-J respectively. With the mode separation, the normal and the common mode admittance $Y_{n,c}$ of the magnet string, which we model as a ladder circuit, can be written down simply as,

$$Y_n = Y_{no} \coth(N\zeta_n) \qquad (1)$$

$$Y_c = Y_{co} \tanh(N\zeta_c) \qquad (2)$$

where Y_{no} and Y_{co} is the characteristic admittance of the ladder circuit. ζ_n and ζ_c and the are expressed by

$$\zeta_{n,c} = \cosh^{-1}(1 + Z_{n,c}Y_{n,c}). \qquad (3)$$

$Z_{n,c}$ is the mode impedance of the magnet and $Y_{n,c}$ is the mode admittance expressed by the capacitance to the ground. Above equations are simple yet very powerful to fully describe the magnet string of resonant feature[2]. The analytic solution in time domain is possible by Inverse Laplace transformation[2]. The admittance of the HIMAC magnet string was measured and the validity of the present model was verified. At the HIMAC the resonance can be suppressed by the bridge resistor parallel to the magnet. This resistor also helps to bypass the ripple and spike current of the magnet, which was verified by observing the voltage induced in one trun coil.

With a finding of the presence of two orthogonal mode in the load, the model of the mode separation is extended to the power supply side. Direct consequence of the preceding argument is the addition of the common mode low pass filter. Without this filter, the common mode ripple voltage is directly applied to the magnet string. Furthermore the common mode current in the HIMAC Bending magnet string does not appear as the magnetic field because of the separate connections of the upper and the lower coils due to the nature of the parallel direction of the current.

In this way, in the HIMAC, most of the ripple voltage of the normal and common mode is suppressed. The relative ripple current of the Quadrupole with active filter was 3 ppm and that of the Bending magnet without active filter was around 5 ppm right after the initial operation. It appeared that the beam spill did not reflect the small ripple content.

III. Improvement at the 50Hz and 100 Hz ripples

The ripple component of 50 Hz and 100 Hz were the main component seen in the output

of the power supply. The fluctuating component of the beam spill appeared to be 100 Hz. 100 Hz is caused by the imbalance of the phases of the AC power line. But 50 Hz can not be generated by the imbalance. These frequencies can not be damped by the low pass filter as the cut off frequency of both mode is chosen to be 75 Hz. Lowering the cut off frequency helps in reducing the ripple but slowing the response of the trapezoid pattern and deteriorating the tracking accuracy between the Quadrupole and the Bending magnet. We decided to strengthen the active filter of the Quadrupole by adding the bandpass filter of 50 Hz and 100 Hz for the individual fine tuning of the phase control. The bandpass filter worked fine as expected and the ripple was reduced. Through the careful study of the 50 Hz source, we found that the 50 Hz is originated from the DCCT. Although the relative amplitude of the DCCT was small as 50 ppm, it has been a performance limiting factor to go below ppm level. With bandpass filter the relative ripple content became at a level of 0.3 ppm for the time in synchrotron power supply history. The main frequency of the beam spill changed from 100 Hz to 50 Hz. We found that the 100Hz was a superposition of the 50 Hz ripple of two different sources whose phases are shifted, namely from the power supply of the Focusing Quadrupole and that of the Bending magnet. The remained 50 Hz came from Bending magnet power supply. The change of tune of the beam is speculated to come indirectly through Sextupole magnet that compensate the chromaticity. This was verified that by reducing the Sextupole strength, the better quality of the beam spill is obtained. With the evidence that the present beam spill is affected by Bending magnet, we decided to reduce the ripple current in the Bending magnet by adding the active filter of the similar type of the Quadrupole power supply. The inductance of the Bending magnet load is six times larger than that of the Quadrupole and supplying larger power is required. Typical reduction of 25 dB at 100 Hz was achieved after an elaborate adjustment of the cut off frequency of the high pass filter that is incorporated in the active filter circuit. Typical example of the frequency spectrum at 600 MeV/u with and without active filter are shown in Fig.2. where 50 Hz is reduced by 28 dB and 100 Hz is 32 dB. The small 50 Hz ripple is also due to the installation of the Holec DCCT. Its linearity and the stability are checked and implimented into the ACR feedback circuit.

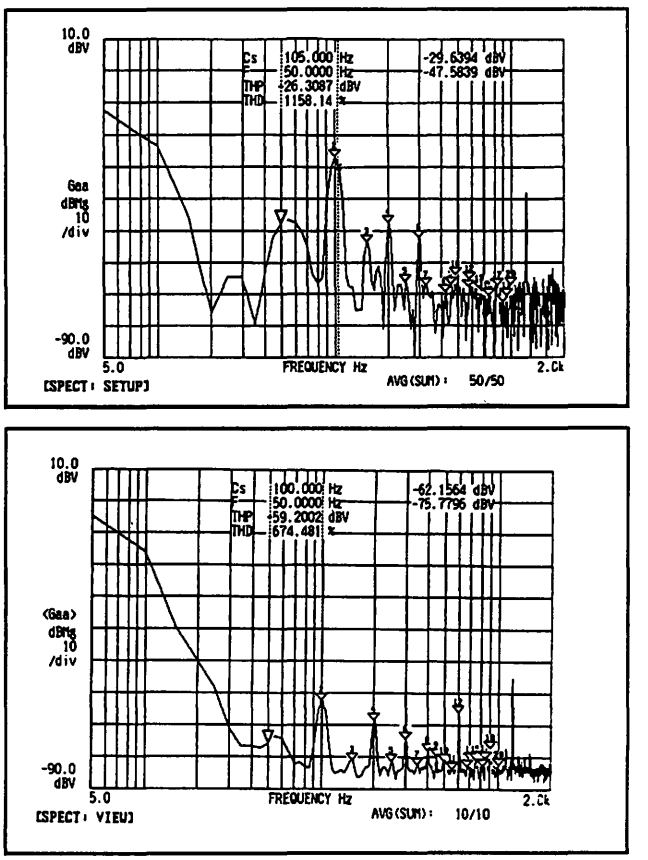

Fig.2 Ripple voltage spectrum of the Bending magnet at 600 MeV/u without (upper graph) and with (lower graph) active filter.

IV. ACKNOWLEDGMENTS

We gratefully acknowledge the support of the members of the division of accelerator physics and AEC. The author thanks the enlightening discussion with Prof.Y.Irie of KEK.

V. REFERENCES

[1] M. Kumada , to be published in NIM
[2] M. Kumada , to be published in particle accelerator .

The optical design of HIMAC secondary beam course

Masahito Hosaka, Koji Noda, Takeshi Murakami, Mitsutaka Kanazawa,
Atsushi Kitagawa, Yukio Sato, Eiichi Takada, Masami Torikoshi
and Satoru Yamada

National Institute of Radiological Sciences
Anagawa, Chiba-city, Chiba-prefecture, 260, Japan

ABSTRACT

A new beam course is under construction in HIMAC, NIRS, in order to utilize radioactive secondary beams for medical purpose. The new course comprises a doubly achromatic spectrometer, which separates projectile fragmentations. The design and the beam optics are presented.

1. INTRODUCTION

Application of radioactive beams[1] is related to vast scientific areas, and one of the fruitful candidates is a medical use. The heavy-ion accelerator complex for medical use, HIMAC, began its operation in 1994 and continues treatment of cancer patients[2]. Great advantages of charged-particle therapy, especially by heavy ions, are the excellent dose distribution and the high biological effectiveness.

Although ranges and scattering angles in various materials can be, in principle, precisely evaluated, small ambiguities are left in evaluation of the dose distribution inside human bodies because they are complicated mosaic of soft and hard tissues. In order to fully utilize the advantage of the charged particles, precise measurements and/or confirmation of dose distribution inside bodies under practical conditions are important. Combination of radioactive secondary beams of positron emitters and annihilation γ-ray detectors like PETs will realize these measurements with no excessive dose. Beams of ^{11}C and ^{19}Ne are good candidates for this purpose and are mainly quoted in the design stage of the new course. On the other hand, other types of beams, especially heavier ones, are taken into consideration in order to expand experimental fields being carried out by the new course. Therefore beam optics of three beam courses are studied in order to maintain the versatility in the future. One of the new courses is now under construction and will be completed in three years. This paper describes design and beam optics of the new course.

2. BEAM OPTICS AND LAYOUT

Layout of the new course A layout of the new course is illustrated in Fig. 1. The new beam course is a double-achromatic fragment separator, comprising two bending magnets, 11 quadrupole magnets, and an energy degrader.

The reaction products produced in the production target, are separated from the primary beam by a 20° bending magnet (BM01). The maximum magnetic rigidity is chosen to be 8.13 Tm, which corresponds to q/A = 1/2 ions with an energy of 600 MeV/nucleon.

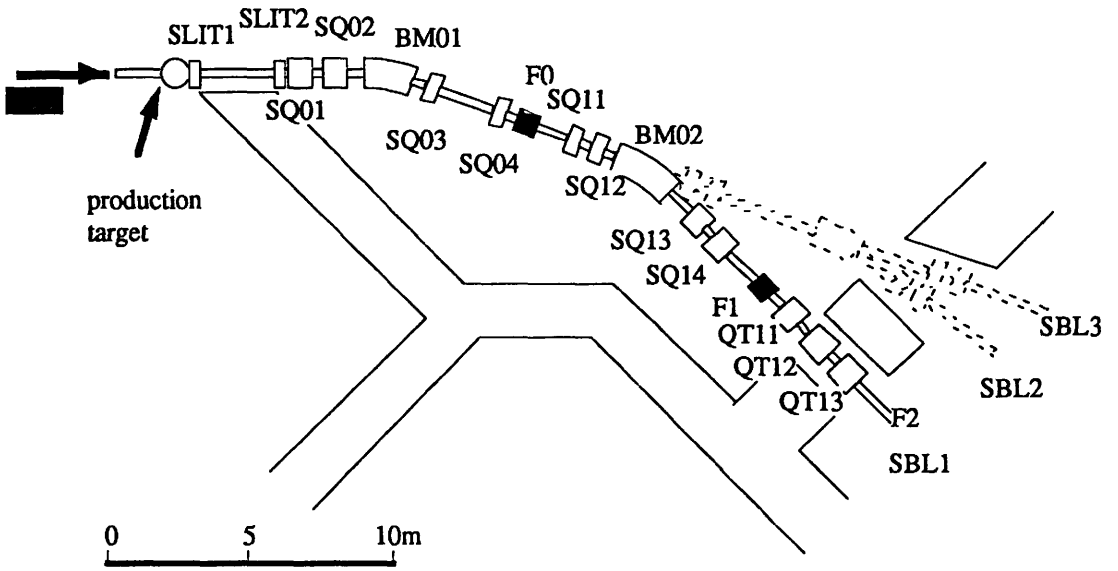

Fig. 1 Layout of HIMAC secondary beam course. The course denoted by " SBL1" is now under construction.

Dumping locations of primary beams vary dependent on its magnetic rigidity relative to that of a secondary beam. Most of primary beams are stopped by a movable beam stopper placed between an exit of the magnet, BM01, and an entrance of a quadrupole magnet, SQ04. The precise separation of the fragments is performed at a dispersive focusing position F0 where the fragments with different magnetic rigidity are focused on the different position. The dispersion D at F0 is taken to be the value of 1.87 (cm/%). With an object size x_0 = ±0.3cm, at the production target, and then at F0 the image size $x = (x,x)x_0$ = ±0.28cm, the momentum resolution is $R = 2x/D$ = 0.30%. An achromatic energy degrader of a wedge in shape can be inserted at F0, which allows an additional fragment separation at the later stage.

The second magnet BM02, with a bending angle of 26.5° and a pair of quadrupole magnets realize the double achromatic condition that two chromatic terms (x,p) and (x',p) vanish hereafter. Thus, the image size of the secondary beam, which is broadened owing to its own momentum spread at the dispersive focus F0, is once more shrunk. When an achromatic energy degrader is placed at F0, an additional isotope separation can be performed at the second focusing point F1. This second selection based on the difference of the atomic energy loss in the degrader, is essential for the separation of fragments of heavier nuclei with whose magnetic rigidity one can not identify.

The three last quadrupole magnets gives the third focus at F2 where radiation of the radioactive secondary beam is performed for medical purpose or for other scientific research. The flexibility of using three quadrupole magnets allow the focusing position to vary to meet various requrments.

As shown in Fig. 1., whole system is not symmetric due to constraint that three beam courses should be made within limited space. Although the optimization process to attain double achromatic condition may need a longer time than that of the symmetric case, it essentially gives the same properties. The beam optics was calculated using the code MAGIC[3]. The design parameters and values of matrix elements are summarized in Table 1 and the first order beam envelope is shown in Fig. 2.

Table 1
The parameters of the secondary beam course

Angular acceptance	
vertical	±13 mrad
horizontal	±13 mrad
Momentum acceptance	±2.5%
Max. magnetic rigidity	8.13 Tm
Flight path length	11.9m to F0
	22.6m to F1
	29.4m to F2

The ion optical matrix elements[a)]

Matrix element	F0	F1	F2
(x,x)	-0.93	0.87	-0.35
(x,x') [cm/mrad]	-0.000	0.000	0.000
(x,p) [cm/%]	-1.87	0.000	0.000
(x',p) [mrad/%]	-0.26	0.000	0.000
(y,y)	-1.75	0.86	-2.1
(y,y') [cm/mrad]	0.029	0.010	0.000

[a)] The matrix elements transfer inital values of x_0, x'_0 and p_0 as following.

$$\begin{pmatrix} x \\ x' \\ p \end{pmatrix} = \begin{pmatrix} (x,x) & (x,x') & (x,p) \\ (x',x) & (x',x') & (x',p) \\ (p,x) & (p,x') & (p,p) \end{pmatrix} \begin{pmatrix} x_0 \\ x'_0 \\ p_0 \end{pmatrix}$$

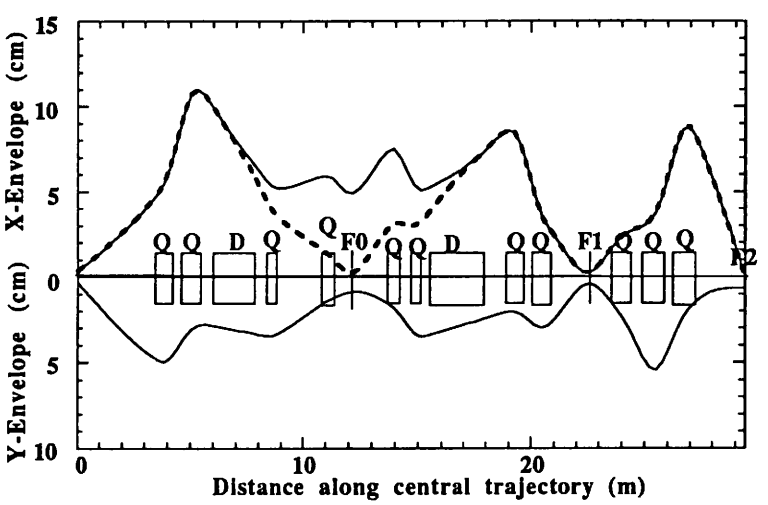

Fig. 2. The first order beam envelopes calculated for a initial parallelogram-like emittance of ±13 mrad in angle and ± 3mm in size

Solid line : with momentum spread ±2.5%
Dashed line : without momentum spread

Acceptance In general large values of beam emittance and momentum spread are unavoidable in secondary beams. Therefore wide acceptance is needed to collect a larger amount of all the fragment. These angular and momentum spread of the secondary beam are estimated based on the statistical model of Goldhaber[4]. Consequently the acceptance values of ±13mrad both horizontal and vertical angle, and ±2.5% in momentum are chosen. With these values, the fragment separator can transport as secondary beam, 65% of ^{11}C and 90% of ^{19}Ne fragments produced in the reaction that a 5cm-thkickness beryllium target are bombarded with 600MeV/nucleon ^{12}C and ^{20}Ne primary beams respectively.

Second order calculation An optics of an ion optical system with a wide acceptance, might be affected by the higher order aberration greatly. Hence we evaluated the second order aberration for the secondary beam course using the code GIOS[5] and the following effects were found. First, the focal plane at F0 is slightly tilted relative to the perpendicular plane to the optical axis. Although this aberration deteriorates the momentum resolution at F0, it was confirmed that degrading of the ability is negligible for the separation of nuclei such as ^{11}C or ^{19}Ne. Second, the image size is found to increase owing to the second order aberration, especially at the focusing points. As an example, the calculated position distribution of the secondary beam of ^{11}C at the second focus F1 is shown in Fig. 3. The secondary beam is assumed to be initially distributed of Gaussian shape in position, angle and momentum space, whose widths are determined under the condition that the secondary beam is produced by a bombardment of a primary beam of 600MeV/nucleon ^{12}C with a 5cm thickness beryllium target. As shown in the figure, the second order aberration does not make much difference to the position distribution of the secondary beam, except for a rather long outer tail. This tail may have a harmful effect for the separation of the fragments with very small production cross section from those with large production cross section, but in most of case the effect is expteced to be of little importance.

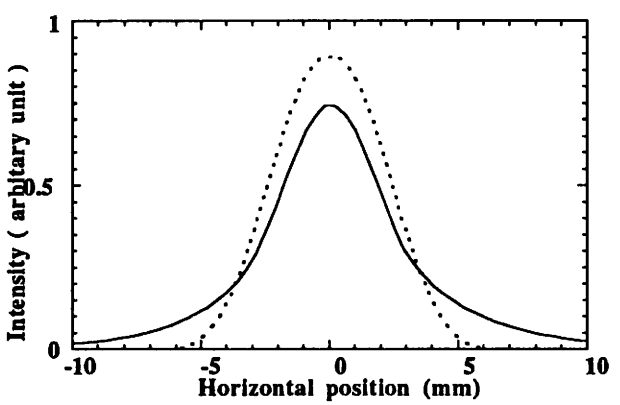

Fig. 3. Calculated ^{11}C beam position distribution at F1.
Solid line : the second order caluculation
Dashed line : the first order calculation

ACKNOWLEGEMENTS

The authors would like to thank Dr. K. Kawachi for his encouragement and helpful advice.

REFERENCES

[1] T. Kubo et. al., Nucl. Insr. and Meth. B70 (1992) 309
[2] K. Sato et. al., Nucl. Phys. A588 (1995) 229c-234c
[3] A. S. King et. al., SLAC-183-RL-75-110 (1975)
[4] A. S. Goldhaber, Phys. Lett. B53 (1974) 306.
[5] H. Wollnik et al., Nucl. Instr. and Meth. A258 (1987) 408.

A TREATMENT BEAM CONTROL SYSTEM FOR IRRADIATION GATED BY RESPIRATION OF A PATIENT

K. Noda, S. Minohara, M. Torikoshi, M. Kanazawa, E. Takada,
N. Araki, A. Noda*, A. Itano**, K. Sato***, H. Ogawa and S. Yamada

National Institute of Radiological Sciences, Chiba 263, Japan
*Institute for Chemical Research, Kyoto University, Uji 611, Japan
**Regional Hygiene Division, Hyogo Prefectural Government, Kobe 650, Japan
***Research Center for Nuclear Physics, Osaka University, Ibaraki 567, Japan

Abstract

A beam control system for irradiation treatment gated by respiration of a patient has been developed at HIMAC to minimize an unwanted irradiation to normal tissues around tumor. The system employs rf-knockout extraction with gate function. Preliminary experimental results, which were carried out with moving phantom and simulating signal of respiration, are encouraging.

1. INTRODUCTION

Clinical trial has been successfully progressing since June 1994, after commissioning of a heavy ion accelerator complex, HIMAC, dedicated to medical applications [1].

A high irradiation accuracy is required in heavy ion therapy because of the high dose localization. In treating a tumor moving along with respiration of a patient, in particular, damage to normal tissues around tumor is inevitable without beam control that gates irradiation according to respiration. A beam delivery scheme, which can respond to irregular respiration, should be applied in order to minimize the unwanted irradiation to normal tissues around tumor. At HIMAC, therefore, such a system has been developed [2,3].

The design considerations and the preliminary experimental results are reported in the paper.

2. BEAM CONTROL SYSTEM

A beam control system for the irradiation gated by respiration requires essential design considerations as follows. (1) Beam extraction method should respond quickly to a trigger signal according to irregular respiration. (2) Operation pattern of synchrotron should give maximum irradiation dose rate. (3) An aborting system of residual beam should be provided in order to avoid undesired activation by unused beam.

2.1 Extraction method

Concerning the irradiation gated by respiration, it is important to start and stop beam extraction promptly according to the beam "on/off" signal. One of the suitable extraction methods for this purpose is beam extraction using a transverse rf field resonated with a horizontal betatron tune, while a separatrix is kept constant, which is called "rf-knockout extraction". The transverse rf electric field is applied with frequency and amplitude modulation. The frequency modulation increases an extraction efficiency because it broadens a frequency band width corresponding to a horizontal tune spread at a resonant extraction. The amplitude modulation is applied to control a spill envelope of an extracted beam. Advantages in the present method are 1) prompt response to start and stop of the beam extraction because of using an rf electric field with a faster response compared with magnetic elements, and 2) a small emittance in the horizontal direction due to a constant separatrix. The results from experiments showed that the response is within 1ms and the horizontal emittance of beam extracted by the present method was reduced by about 70% compared with that by the ordinary extraction method. The extraction efficiency in the present method was more than about 85% which was comparable with that in the ordinary method. The details were reported in Ref. [2].

2.2 Operation pattern of synchrotron

To optimize an operation pattern of synchrotron, it is assumed that a respiration pattern is independent of an operation pattern of synchrotron, and an irradiation for treatment is continued infinitely. Under the condition, an irradiation dose rate is maximized at an extraction duty factor of 50%, because a beam can be extracted as long as the extraction period is coincident with an irradiation period permitted by the respiration pattern. If the extracted beam intensity can be infinitely increased, on the other hand, the dose rate is increased as increasing the duty factor. At HIMAC, therefore, the dose rate is maximized at the duty factor of 50% in the 0.3Hz operation of synchrotron. The effective dose rate in this operation can be kept at the operational value if the extracted beam intensity is increased by 70%, which will be easily realized.

All of the accelerated beam should be extracted

as soon as the extraction signal is generated, to reduce effective irradiation period. On the other hand, an irradiation period more than 10 times longer than that of wobbling magnets is required to obtain a uniform dose in the lateral distribution. The amplitude of a transverse rf field is determined so that all of the accelerated beam is extracted during about 400ms in order to satisfy the above requirements.

2.3 Beam aborting system

In the irradiation gated by respiration, the residual beam has to be aborted around synchrotron, because the accelerated beam should not be extracted from synchrotron as long as a "beam off" signal is generated. Decelerating the residual beam to an injection energy as a beam aborting system is proposed to avoid unwanted activation around synchrotron. As a result of the preliminary test, the deceleration efficiency was about 80%. Details will be presented elsewhere[4].

Summarizing the above considerations, an operation patten of the beam control system for the irradiation gated by respiration is schematically shown in Fig. 1.

3. EXPERIMENTAL RESULTS

An irradiation gated by respiration was preliminarily experimented by using a phantom moving along with a simulating signal of respiration [3]. In the experiment, synchrotron is operated by a cycle of 0.3Hz with a duty factor of 45%. Carbon beams with the energy of 290 and 400MeV/n are extracted from synchrotron by the rf-knockout method, and delivered through an irradiation system to an isocenter at a treatment room. Concerning the experimental setup in the treatment room, a phantom placed at the isocenter is moved with a stroke of 25mm and, is driven by a 0.33Hz sinusoidal signal that pretends respiration. The simulating signal is generated by a sensitive strain gauge set on the phantom. A collimator with an aperture of 40mm square is placed in front of the phantom in order to define an irradiation field, and is 450mm distant from the phantom.

Figure 2 shows a typical result of a beam extraction gated by the simulating signal. As can be seen in the figure, the beam was successfully extracted in only the permitting irradiation period. A penumbra size was also obtained by measuring a density of an exposed X-ray film attached with the phantom moving along with the simulating signal. Three cases, i.e, a fixed phantom, a gated irradiation to moving phantom, and an ungated irradiation to moving phantom were investigated as shown in Fig. 3. The penumbra size P_{80-20} in three case were obtained as 2.4, 6.1 and 19.4mm, respectively, where P_{80-20} is defined at the distance of the lateral dose falloff from 80% to 20%. The P_{80-20} in the fixed phantom is naturally less than that in the gated irradiation, because the phantom in the latter case moves somewhat during the irradiation due to applying a sinusoidal wave as the simulating signal. However, the P_{80-20} in the gated irradiation is considerably reduced to 6.1mm from 19.4mm in the ungated irradiation.

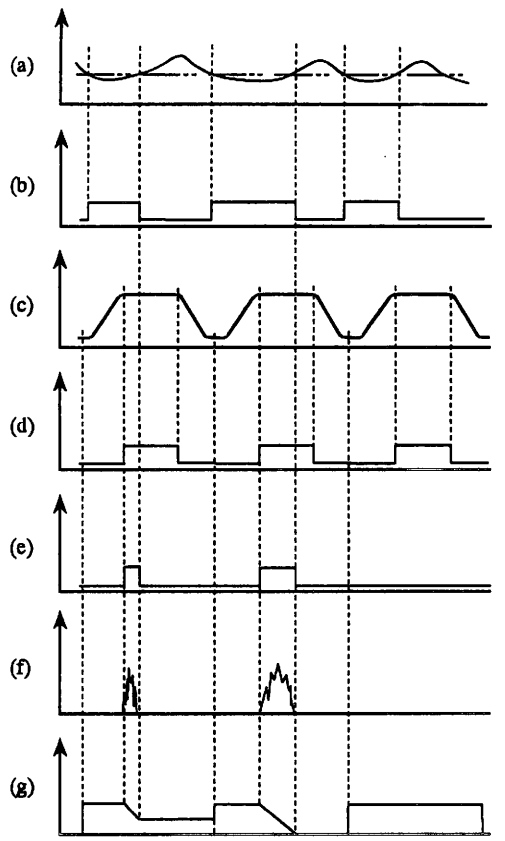

Fig. 1 Schematic operation pattern of the system for irradiation gated by respiration. (a) Respiration signal, (b) Permitting irradiation signal, (c) Operation pattern of synchrotron, (d) Flat-top signal, (e) Extraction signal, (f) Beam spill, (g) Circulating beam intensity.

4. CONCLUSION

The beam control system for irradiation treatment gated by respiration is developed. The beam control system's ingredients are; rf-knockout extraction that can respond to a respiration signal quickly, a 0.3Hz, 50% duty operation of synchrotron that maximizes dose rate, and a beam deceleration as a beam aborting system.

As preliminary results of experiment, an extraction gated by a simulating signal of respiration was successfully achieved. The penumbra size was also measured by using a phantom moved along with the simulating signal, and was considerably reduced to 6.1m from 19.4mm in the ungated irradiation. The system will play an important role in clinical study such as treatment for a lung or liver cancer moved along with respiration of a patient.

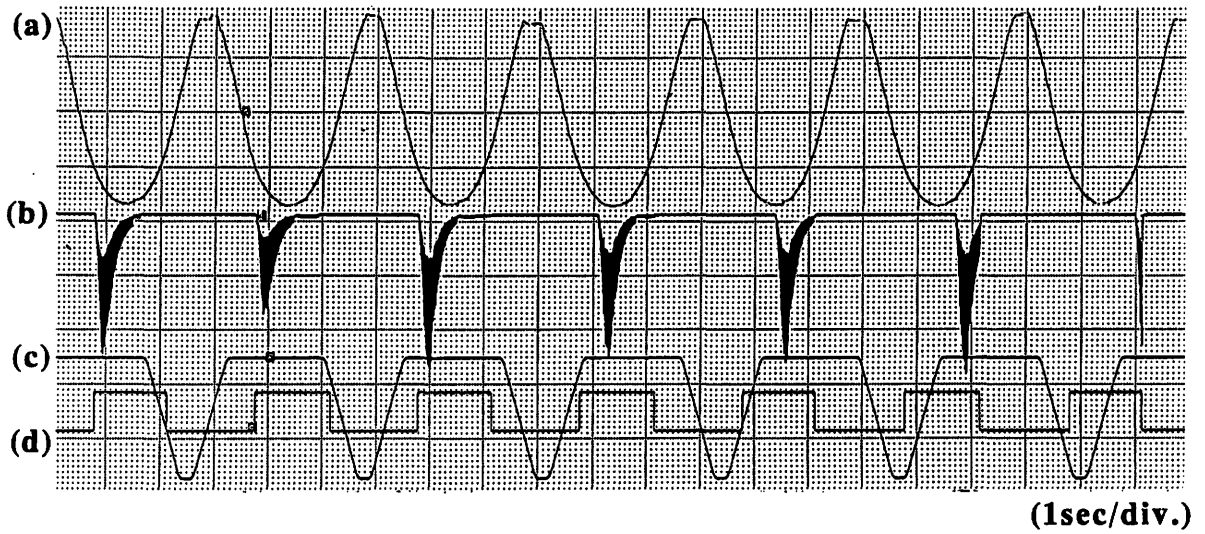

Fig. 2 Beam extraction gated with the simulating signal of respiration in 400MeV/n carbon beam.
(a) Simulating signal of respiration, (b) Beam spill, (c) Operation pattern of synchrotron, (d) Permitting irradiation signal.

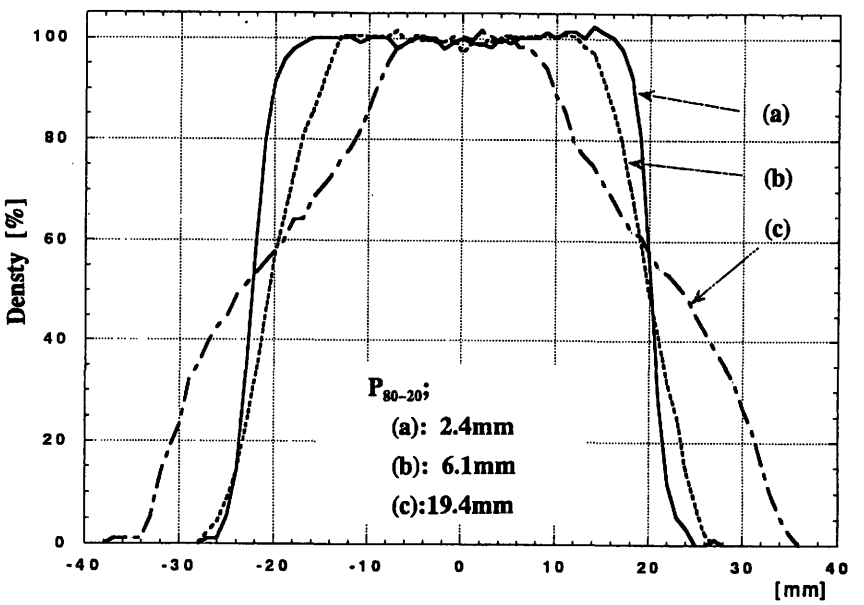

Fig. 3 The lateral dose distribution in 290MeV/n carbon beam. (a) fixed phantom, (b) gated irradiation to moving phantom, (c) ungated irradiation to moving phantom.

5. ACKNOWLEDGEMENTS

The authors would like to express their thanks to MD. H. Kato and Mr. T. Ishii of Division of Radiation Medicine, and Mr. A. Fukumura of Division of Radiation Research at NIRS for valuable discussions. They are also grateful to the crew of Accelerator Engineering Corporation for skilful operation of HIMAC and to Dr. K. Kawachi and members of the Division of Accelerator Physics and Engineering at NIRS for their warm support and encouragement.

6. REFERENCES

[1] K. Sato et al., Nucl. Phys. A588,229(1995).
[2] K. Noda et al., Proc. 4th EPAC, London, 1994, pp.982–984.
[3] S. Minohara et al., Proc. 12th JAMP, Tokyo, 1995, pp.38, in Japanese.
[4] M. Kanazawa, et al., to be submitted.

DEVELOPMENT OF 3–DIMENSIONAL IRRADIATION SYSTEM FOR HEAVY–ION RADIATION THERAPY

Yasuyuki FUTAMI, Hiromi TOMURA, Naruhiro MATSUFUJI and Tatsuaki KANAI

Division of Accelerator Physics and Engineering, National Institute of Radiological Sciences,
9–1, Anagawa 4–chome, Chiba–shi, 263 Japan

Abstract

A three–dimensional irradiation system using a broad beam was installed at HIMAC facility for a heavy–ion radiation therapy. The thickness of the wedge absorber and the shape of the radiation field made by the multi–leaf collimator were changed during irradiation in order to sweep the Bragg peak only in the target area. In this report we discuss the three–dimensional irradiation system of HIMAC and also results of preliminary irradiation tests using ^{12}C beams.

1 Introduction

It is one of the most important goal of any radiotherapy to shape the treatment volume as exactly as possible to the tumor as the target volume. In most cases a sharp cutoff of the dose is needed in order to spare the surrounding healthy tissue or critical structures to a maximum extent. It is necessary to use a flat–top depth–dose distribution extending several centimeters, even tens of centimeters to encompass solid tumors. For this purpose heavy ion beams are delivered to the treatment volume by the beam scanning method [1] or the broad beam method. The clinical port at HIMAC facility is designed by the latter method and shown in fig.1. The system consists of a pair of wobbler magnets (a), a scatterer (b), a ridge filter (c), a range shifter (d), a pair of wedge absorber (e), a multi–leaf collimator (f), a compensator (g) and a monitor system. The wobbler magnets and the scatterer are used for spreading the beam uniformly over the radiation field[2]. For 2–dimensional irradiation, the ridge filter is used to spread the sharp pristine Bragg peak. A spread–out Bragg peak (SOBP) is made by superposing shifted Bragg peaks with suitable superposing ratio. Irregular shape of radiation fields are obtained by blocking the uniform beam with the multi–leaf collimator. Fine adjustment of heavy ion range in patient is performed by the range shifter. And the compensator is used for adjusting position of the distal part of the target.

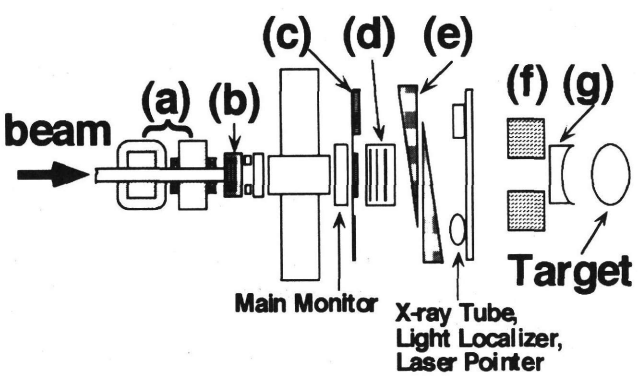

Figure 1: Schematic diagram of HIMAC irradiation port. Devices labeled (a)~(g) are explained in text.

For a tumor conform treatment, a 3–dimensional irradiation using a synchronized fast sweeping technique is also possible in HIMAC irradiation system and presently developed. This novel technique implies some important advantages. The 3-dimensional dose distribution can be shaped exactly to the tumor volume in order to prevent particles from depositing their biologically very effective dose outside the target volume. Using the sweeping technique, complex 3-dimensional scanning procedure is no longer needed saving irradiation time. And the system can be extended from the present 2-dimensional irradiation system reducing the costs. In the following the principles of the 3–dimensional irradiation are discussed and the first results obtained with the system at HIMAC are presented.

2 Method of 3D irradiation

Figure 2 illustrates the 3-dimensional irradiation system installed in HIMAC. An uniform beam is

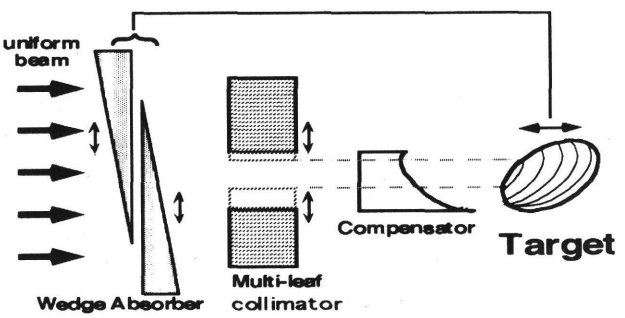

Figure 2: Illustration of Three–Dimensional Irradiation.

DEVELOPMENT OF 3–DIMENSIONAL IRRADIATION SYSTEM FOR HEAVY–ION RADIATION THERAPY

Yasuyuki FUTAMI, Hiromi TOMURA, Naruhiro MATSUFUJI and Tatsuaki KANAI

Division of Accelerator Physics and Engineering, National Institute of Radiological Sciences,
9–1, Anagawa 4–chome, Chiba–shi, 263 Japan

Abstract

A three–dimensional irradiation system using a broad beam was installed at HIMAC facility for a heavy–ion radiation therapy. The thickness of the wedge absorber and the shape of the radiation field made by the multi–leaf collimator were changed during irradiation in order to sweep the Bragg peak only in the target area. In this report we discuss the three–dimensional irradiation system of HIMAC and also results of preliminary irradiation tests using ^{12}C beams.

1 Introduction

It is one of the most important goal of any radiotherapy to shape the treatment volume as exactly as possible to the tumor as the target volume. In most cases a sharp cutoff of the dose is needed in order to spare the surrounding healthy tissue or critical structures to a maximum extent. It is necessary to use a flat–top depth–dose distribution extending several centimeters, even tens of centimeters to encompass solid tumors. For this purpose heavy ion beams are delivered to the treatment volume by the beam scanning method [1] or the broad beam method. The clinical port at HIMAC facility is designed by the latter method and shown in fig.1. The system consists of a pair of wobbler magnets (a), a scatterer (b), a ridge filter (c), a range shifter (d), a pair of wedge absorber (e), a multi–leaf collimator (f), a compensator (g) and a monitor system. The wobbler magnets and the scatterer are used for spreading the beam uniformly over the radiation field[2]. For 2–dimensional irradiation, the ridge filter is used to spread the sharp pristine Bragg peak. A spread–out Bragg peak (SOBP) is made by superposing shifted Bragg peaks with suitable superposing ratio. Irregular shape of radiation fields are obtained by blocking the uniform beam with the multi–leaf collimator. Fine adjustment of heavy ion range in patient is performed by the range shifter. And the compensator is used for adjusting position of the distal part of the target.

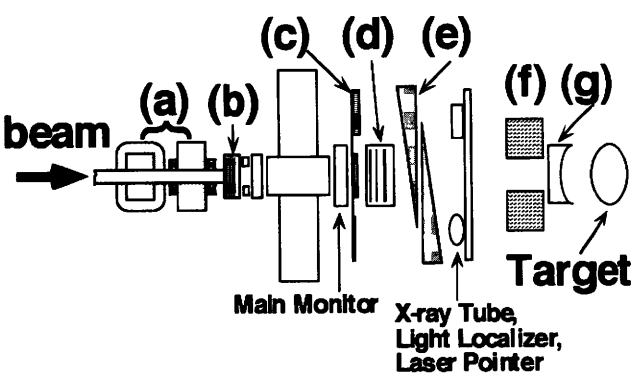

Figure 1: Schematic diagram of HIMAC irradiation port. Devices labeled (a)~(g) are explained in text.

For a tumor conform treatment, a 3–dimensional irradiation using a synchronized fast sweeping technique is also possible in HIMAC irradiation system and presently developed. This novel technique implies some important advantages. The 3-dimensional dose distribution can be shaped exactly to the tumor volume in order to prevent particles from depositing their biologically very effective dose outside the target volume. Using the sweeping technique, complex 3-dimensional scanning procedure is no longer needed saving irradiation time. And the system can be extended from the present 2-dimensional irradiation system reducing the costs. In the following the principles of the 3–dimensional irradiation are discussed and the first results obtained with the system at HIMAC are presented.

2 Method of 3D irradiation

Figure 2 illustrates the 3-dimensional irradiation system installed in HIMAC. An uniform beam is

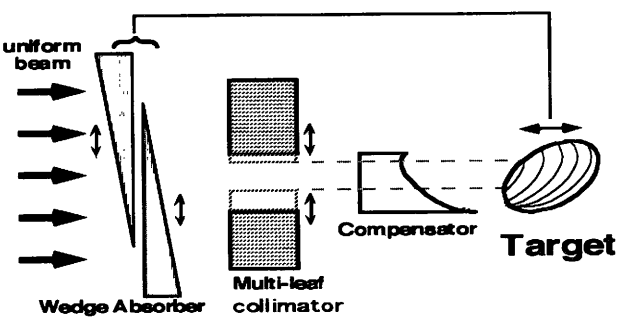

Figure 2: Illustration of Three–Dimensional Irradiation.

made by the wobbler magnets and the scatterer in the same way of the 2-dimensional irradiation. "Slightly" spread-out Bragg peak (we call it s–SOBP in this paper) is made by the ridge filter. The s–SOBP is shifted by inserting the wedge absorbers in the beam course. By combination of the two wedge absorbers, the total thickness of the absorber is uniform in the radiation field. A SOBP that should be conformed to a target shape (we call it total–SOBP in this paper) is made by superposing shifted s–SOBP by changing the absorber thickness during the irradiation with suitable superposing ratio. During the sweep of the s–SOBP in the target region, needless part of the irradiation field can be cut by adjusting the irradiation field with the multi–leaf collimator.

In order to realize this conformation therapy, we have to develop the fast movements of the wedge absorbers and the multi–leaf collimator and their synchronism. Specifications of the wedge absorber and multi–leaf collimator installed at HIMAC are shown in fig.3.

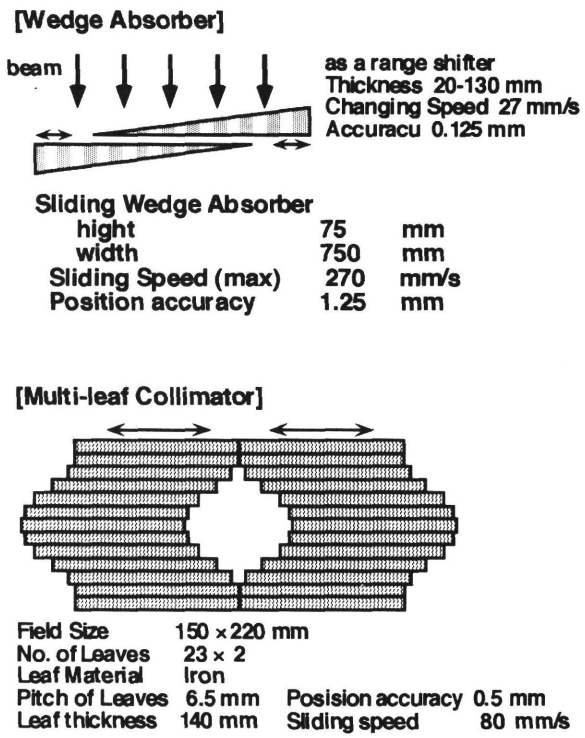

Figure 3: Specification of wedge absorber and multi–leaf collimator.

3 Measurement of dose distribution

The first test of the 3–dimensional irradiation confirming with eyes was carried out using 290 MeV/n carbon beam. The target volume was assumed to be a ball of 7 cm in diameter, which is embedded in Polymethyl methacrylate (PMMA) material. To monitor the beam profile in the target material, a ZnS screen was inserted between PMMA blocks and placed almost parallel but slightly tilted to the beam direction. The movements of the wedge absorbers, the multi–leaf collimator and also the beam profile along the beam axis were recorded by video camera. In each slice scintillation light from the Zns screen lay almost within the target area and results were satisfactory.

For the quantitative test of the performance of the 3–dimensional irradiation, a depth dose distribution was measured for 10 cm width total–SOBP using 290 MeV/n carbon beam. The SOBP was designed to make a uniform biological dose distribution[3] using a thick ridge filter (ridge filter A). The 5 mm width s–SOBP was made by a thinner ridge filter (ridge filter B) that was used to make a uniform biological dose distribution. Three types of radiation fields were made:

(a) 10 cm width SOBP directly made by 2D irradiation using the ridge filter A

(b) 5 mm width SOBP made by 2D irradiation using the ridge filter B

(c) 10 cm width total–SOBP made by 3D irradiation using ridge filter B.

In each irradiation the physical dose was measured with a standard ionization chamber. The preliminary results for the depth dose distribution are shown in fig.4. Open circles, diamonds and closed circles

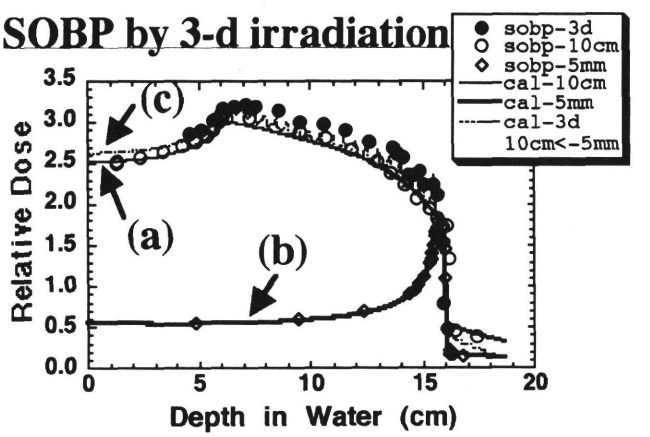

Figure 4: Measured and calculated physical dose distributions.

represent measured physical dose of (a), (b) and (c), respectively. Lines are calculated depth dose distribution[3]. The measured dose by 3D irradiation were slightly larger than those by 2D irradiation. However, measured and calculated results by 3D irradiation were agreed among themselves. This shows that the total–SOBP realized by 3–dimensional irradiation method can be improved by optimizing the shape of the s–SOBP.

To reproduce the 2D SOBP ((a) in fig.4) using the 3D irradiation, a new ridge filter for the modulated s–SOBP of 5 mm in width was designed. Figure 5 shows the calculated results for the physical dose distribution. It is seen that the total–SOBP of the mod-

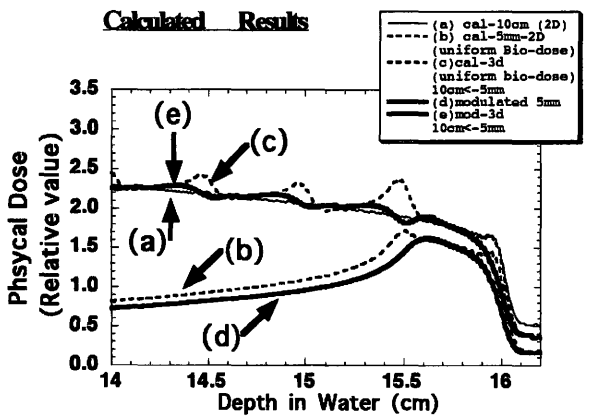

Figure 5: Calculated physical dose distributions (a) for 10 cm field by 2D only, (b) for 5mm uniform biological dose distribution, (c) for 10 cm field by 3D with (b), (d) for modulated 5mm field, (e) for 10 cm field by 3D with (d).

ulated ridge filter is closer to the 2D results (within ± 4.6 %) than those of the ridge filter *B*. Needless to say that the further study is needed to optimize the shape of the s–SOBP and other test experiments using the 3–dimensional irradiation method with the modulated ridge filters are planed. In order to evaluate the quality of the radiation field made by the 3–dimensional irradiation (uniformity, penumbra), the monitoring systems for the dose distribution have to be developed. For this purpose we have planed to develop a proportional chamber (for 1–dimensional distribution), a silicon strip detector (for 2–dimensional distribution) and a pile of ionization chambers (for 3–dimensional distribution).

4 Concluding remarks

An irradiation system of 3–dimensional conformation therapy was designed and installed at HIMAC facility. The 3–dimensional irradiation for a ball shaped target of 7 cm diameter was performed using 290 MeV/n carbon beam. The wedge absorbers and the multi–leaf collimator were controlled satisfactorily during the irradiation for conformation therapy. Preliminary results of a dose distribution of the 10 cm SOBP made by superimposing 5mm width SOBP using the sliding wedge absorbers was obtained to check the function of the wedge absorbers.

In order to improve this system, we plan to develop the optimizing methods to design a ridge filter and the dose measurement methods.

The authors would like to thank the other members of Division of Accelerator Physics and Engineering of NIRS for their helpful collaboration. They are also indebted to the staff of Accelerator Engineering corporation for their support.

References

[1] Th. Haberer et al., *Nucl. Inst. Meth.* **A330** (1993) 296.

[2] H. Tomura et al., Proc. 10th Sympo. on Accelerator Science and Technology, Hitachinaka, October, 1995.

[3] T. Kanai et al., *NIRS HIMAC report* **HIMAC003** (1992) 1.

PHYSICAL STUDIES OF BEAM DELIVERY SYSTEM FOR PROTON AND HEAVY ION TREATMENT

Akio Higashi, Tatsuaki Kanai*, Hiromi Tomura*, Masahiro Endo*,
Akifumi Itano, Hiroshi Karashima and Yoshio Hishikawa

Charged Particle Treatment, Public Health and Environment Department,
Hyogo Prefectural Government, Kobe, Hyogo, Japan
*Research Center of Charged Particle Therapy, National Institute of Radiological Sciences,
Chiba, Japan

Abstract

We report design and optimization of beam delivery system for proton and heavy ion particles, which will be constructed in charged particle therapy facility in Hyogo Prefecture. Penumbra sizes were calculated for different systems to optimize device parameters under considering effects of multiple scattering and energy loss of beam. It was found that penumbra size of carbon ion beam was about three times smaller than that of proton, and that devices which affect physically in particle delivery system should be placed as upstream as possible to reduce penumbra size.

1. Introduction

It is reported here the results of physical investigation for beam delivery system using proton and heavy ion beam to construct facility of charged particle therapy in Hyogo Prefecture. In this facility, the three fixed beam ports which deliver proton and heavy ion (helium and carbon) beam and a rotatable gantry using proton are planned for treatment issue. The beam delivery system which include such beam ports and gantry have not yet been constructed in Japan.

In the design of the beam delivery system, important devices are wobbler magnets, scatterers, ridge filters and range shifters, because they scatter beam particles and affect penumbra size. Position of these devices are investigated, assuming sizes of the devices which are slightly different from those used in Heavy Ion Medical Accelerator in Chiba (HIMAC) in National Institute of Radiological Sciences (NIRS) but structures of them are almost same as those in HIMAC. Penumbra of the delivery systems which were designed under specification were calculated. Since it is necessary for accurate treatment that penumbra are to be as small as possible, the goal of their size is about 2 mm.

2. Design of the beam delivery system and calculation for penumbra designed

In calculating penumbra, the method developed in NIRS was employed. Physical meaning of the calculation is as follows[1]. Particle distribution is obtained as an approximated solution of the Boltzmann equation. In this case, multiple scattering and energy loss are assumed when particles pass through material in the devices of the delivery system. Fermi and Eyges showed that radial deflection y and its angle ϕ of the particles passing through materials under those assumptions could be calculated[2]. At the formulation, the quantity D which corresponds to the emittance squared in the beam transport are to be written as

$$D = \langle y^2 \rangle \langle \phi^2 \rangle - \langle y\phi \rangle^2,$$

where $\langle y^2 \rangle$ and $\langle \phi^2 \rangle$ are the variances of y and ϕ, respectively and $\langle y\phi \rangle$ is cross term. It is important that effects of multiple scattering and energy loss are already included in them. D is calculated by $\langle y^2 \rangle$, $\langle \phi^2 \rangle$ and $\langle y\phi \rangle$ which are values on the material at each grid point segmented small enough along the beam direction. Penumbra P_{80-20} are to be written as follows;

$$P_{80-20} = 1.68\ \sigma_\phi L_c,$$
$$\sigma_\phi^2 = D/\langle y^2 \rangle + \langle y^2 \rangle \left(\langle y\phi \rangle / \langle y^2 \rangle - 1/L_w \right)^2,$$

where L_c and L_w are the distances from isocenter to collimator and wobbler magnet, respectively. Here the quantitative definition of the penumbra is the distance between 80 % dose point compared to the dose of isocenter and 20 % point of that on lateral dose distribution. This calculation method have much advantage for its analytically solved results than the usually used Monte-Carlo method, because it is easy to understand about the effect of positions of the devices and materials and takes much less times to calculate. For example of position of the devices, it is important to place a collimator to a patient body as close as possible. The results of this method for beam delivery systems in HIMAC have been found to agree within 1 mm or less, which is about 10 % of the penumbra size measured by X-ray photograph.

Figure 1 shows an example of fixed beam port used for proton and heavy ion beam. Calculations for this system were made for 165 and 230 MeV energies of proton and 320 MeV/u energy of carbon ion beam. Figure 2 shows an example of rotatable gantry for proton only. Calculations for this gantry

were made for 165 MeV energy of proton beam. Maximum range of each kind of beam through these delivery systems are about 17 cm for both 320 MeV/u carbon ion and 165 MeV proton beam and about 30 cm for 230 MeV proton, respectively. Distance, L_c, between collimator and isocenter was set to be 40 cm.

3. Results and discussions

Firstly, for the fixed beam delivery system shown in the Figure 1, field radius, maximum range and spread out Bragg Peak (SOBP) width were set to be same in carbon ion and proton beam. The maximum range and SOBP width were taken as 17 cm mentioned above and 6 cm, respectively. Dependence of penumbra size on field radius which was adjusted by scatterer thickness and radius of wobbler were estimated. It was found that the dependence was small but the absolute value of penumbra in the case of proton beam were about three times larger than those of carbon ion beam in the same range. The results are shown in Figure 3. It was also demonstrated that the heavier ion, such as carbon, can perform more accurate treatment.

In next step, effects of scattering in compensator and inside of a patient body were estimated. For simple studies, water was placed after a collimator and its thickness was changed. Water is often used in estimation of scattering in compensator and human body, because density of water is almost the same as polyethylene which is the material of compensator and as a human body. Figure 4 shows the dependence of penumbra size on water thickness in this calculation. It was found that the size of penumbra caused by scattering in the body was smaller than that by the delivery system. It was also shown that the effect of scattering in the compensator was much smaller than that in the body because of difference of path length. As is in the Figure 3, absolute penumbra size of proton beam in the Figure 4 was also found to be about three times larger than that of carbon ion.

In the last study, penumbra size was calculated by changing the position of ridge filter in the gantry shown in the Figure 2 for proton. The results are shown in Figure 5. It can be seen that the distance between scatterer and ridge filter is longer, the penumbra size is larger. The dependence of penumbra size on the positions of devices which scatter beam particles is not only for ridge filter position but also for those of scatterer and range shifter. Scatterer, ridge filter and range shifter should be placed closely each other and as upstream as possible, and the distance from range shifter to the isocenter is to be taken as long as possible. However, it is much difficult in working upon the ridge filter, because the thickness and gaps of the ridges should be much smaller. Selection for material which is easily worked upon or oscillating bar ridge filter and rotating spiral ridge filter are to be taken into account.

Three-dimensionally conformed (3-D) irradiation system is under planning in this facility, because it has much advantage for dose localization. Searching parameters of devices in beam delivery system for adjusting irradiation field can also be simplified using the 3-D system. Dynamic 3-D system without devices which scatter particles and absorb energy of the beam will be installed in this facility to use maximum range of initial beam energy and minimum penumbra size by initial emittance.

References

1) H. Tomura et al., Abstract Book of the Fifth Workshop on Heavy Charged Particles in Biology and Medicine, GSI (1995).

2) L. Eyges, Phys. Rev. 74 (1948) 1534.

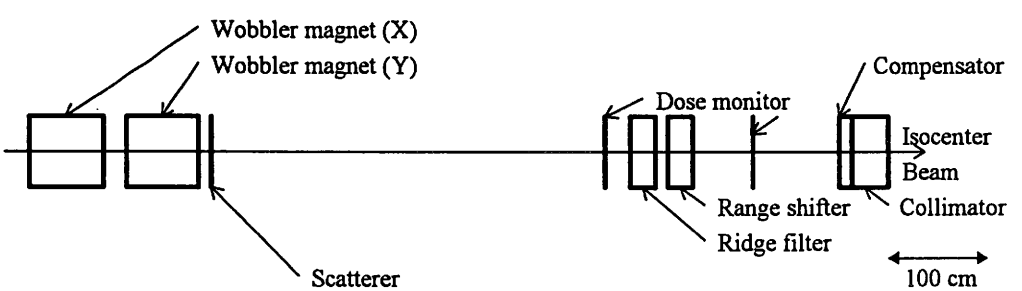

Figure 1. Fixed beam delivery system for proton and heavy ion beam . Total length shown here is 940 cm.

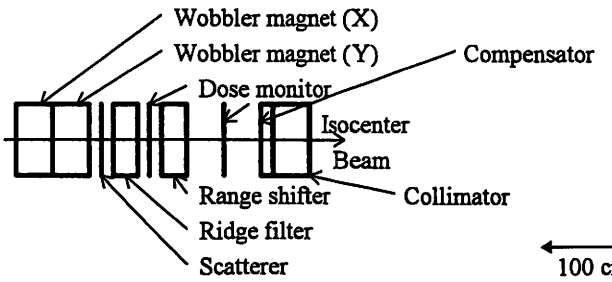

Figure 2. Rotatable gantry for proton beam . Total length shown here is 350 cm.

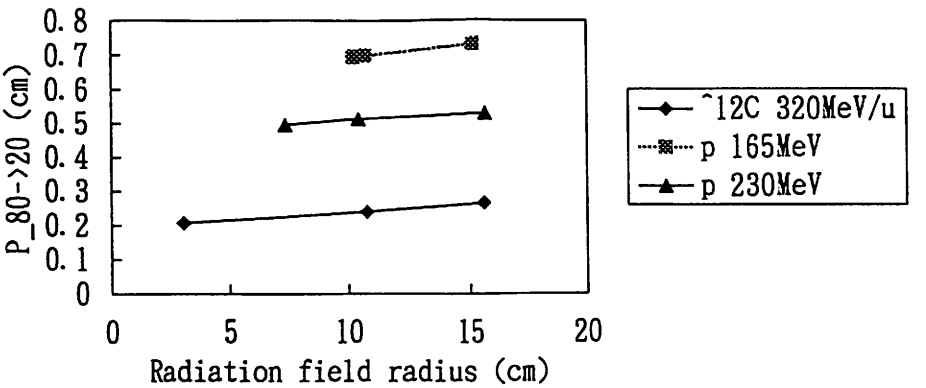

Figure 3. Dependence of penumbra size on field radius at 6 cm of SOBP width.

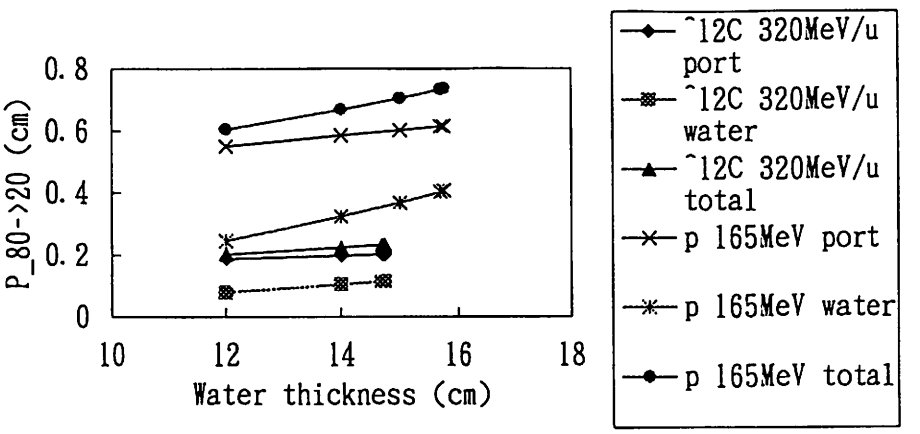

Figure 4. Dependence of penumbra size on water thickness. Water is placed downstream of collimator.

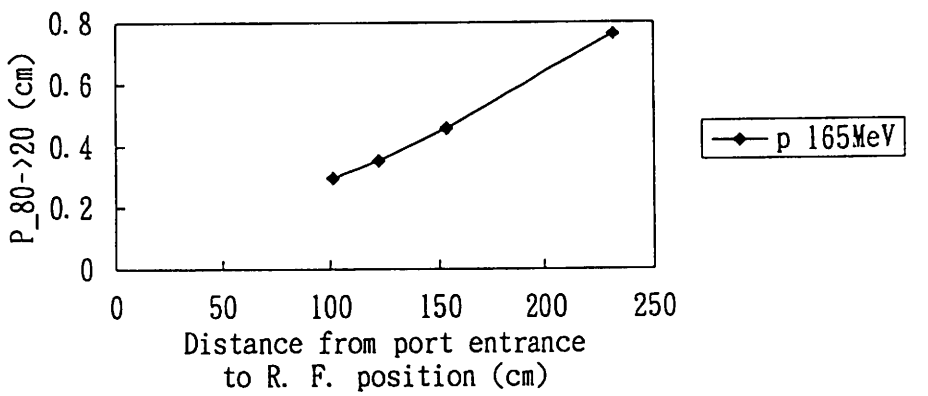

Figure 5. Dependence of penumbra size on ridge filter position in gantry for proton.

DOSIMETRY SYSTEM FOR HEAVY-ION RADIOTHERAPY

Tatsuaki KANAI, Yasuyuki FUTAMI, Hiromi TOMURA and Naruhiro MATSUFUJI

Division of Accelerator Physics and Engineering,
National Institute of Radiological Sciences,
9-1, Anagawa 4-chome, Inage-ku, Chiba-shi, 263 CHIBA JAPAN.

Abstract

This paper describes a dosimetry system for the heavy-ion radiation therapy installed at HIMAC facility. Daily check of the dose monitor, a species of the accelerated particles, their energy are carried out every morning. And the dose calibration of the monitor for each patient condition are also carried out every morning. The variations of the monitor responses were less than 2 % during 3 months of treatment term. In order to shorten the time for the check, a simplified dosimetric system for the dose calibration of the monitor was installed from this autumn.

1. Introduction

A radiation therapy using a carbon beam has been started at HIMAC facility from last year[1]. The heavy-ion radiotherapy is expected to be superior to the conventional radiation because of its excellent dose localization and its high biological effectiveness. Then, it is important to irradiate patients as previously planned by a treatment planning system. Around 18 times of exposures are given to the same patient in the heavy-ion radiotherapy. And it takes over one month to finish the treatment. It is necessary to guarantee daily exposure dose to be the planned exposure. In order to guarantee these things, the check of the dose monitor, a species of the accelerated particles, and their energy are carried out every morning. The dose calibration of the monitor for each patient condition are also carried out every morning. These check is very important for the assessment of the irradiation port.

In this paper, the dosimetry system for the heavy-ion radiation therapy installed at HIMAC facility is presented and discussed in detail.

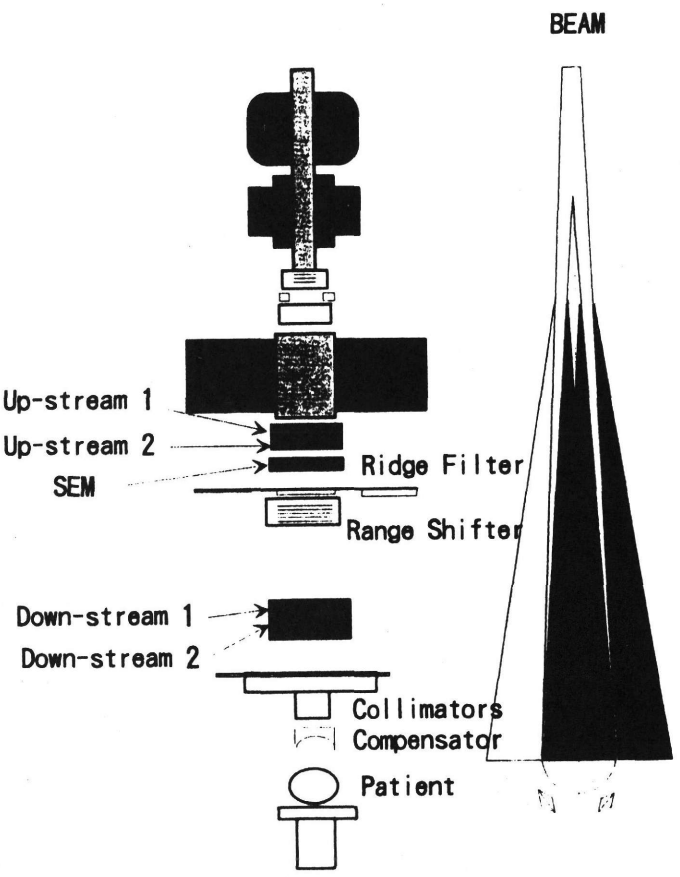

Fig. 1. Illustration of the therapeutic beam port

2. Monitor system

In the HIMAC irradiation course for the radiation therapy, 5 monitors are installed. Fig. 1. shows the illustration of the therapeutic beam port of HIMAC and indicates the location of the monitors in the beam course[2]. Monitors which are shown as up-stream 1,2 and down-stream 1,2 are the parallel plate ionization chamber. The up-stream chamber has two signal electrodes and three high voltage electrodes of the parallel plate ionization chamber. The one signal is fed into a high-

speed amplifier and used for monitoring the time structure of the beam. The other output signal is fed into I/F converter which output a pulse for every 1000 pC. The pulse train is input to a preset counter which is connected to a beam shutter for controlling the exposure dose to the patients. We have another dose controlling monitor, SEM (Secondary Emission Monitor). We have anxiety that beams may have a big spike in the beam spill. In that case, accurate dose can not be measured by the ionization chamber monitor because of recombination effects in the big spike. Then, we used the secondary emission chamber for the back-up of the ionization chamber.

At just up-stream of the beam collimator, a down-stream monitor was placed. The monitor is also a parallel plate ionization chamber, and has one signal plane which is sandwiched by two high voltage electrodes. On one side of the signal plane, there are 29 signal electrodes of 20 mm in diameter which are distributed in the guard earth. This ionization chambers are used for roughly monitoring the uniformity of the irradiation field. The other side of the signal plane of the down-stream chamber is a signal electrode which cover the whole uniform irradiation field. This output is used as another back-up monitor of the exposure dose.

Using these monitor system, the irradiation dose to the patients are controlled and monitored.

3. Dose calibration system

Standard procedure of the dose calibration using the above system is as follows;

1) Depth dose distribution of a spread Bragg peak which has 6 cm width is measured by a standard dosimeter. The standard dosimeter is a parallel plate ionization chamber, which is fabricated by Far West Technology, Co.,. We use a binary filter to change a depth in water in the measurements of the depth dose distributions. The binary filter consists of 9 PMMA (Polymethyl methacrylate; Lucite) sheets of 0.5, 1, 2, 4, 8, 16, 32,64 and 128 mm thickness and 10 x 10 cm area. Inserting these sheets in the beam course, the target thickness is changed. The thickness of the PMMA is transferred to water equivalent thickness.

2) The measured dose distribution is compared with a calculated depth dose distribution. From the comparison, variations of the residual range of the carbon beam at the irradiation site and absolute value of the output of the standard chamber are recorded for the check of the beam energy, and the species of the particles. Fig.2 shows the variation of the range of the 350 MeV/u carbon beam checked by the

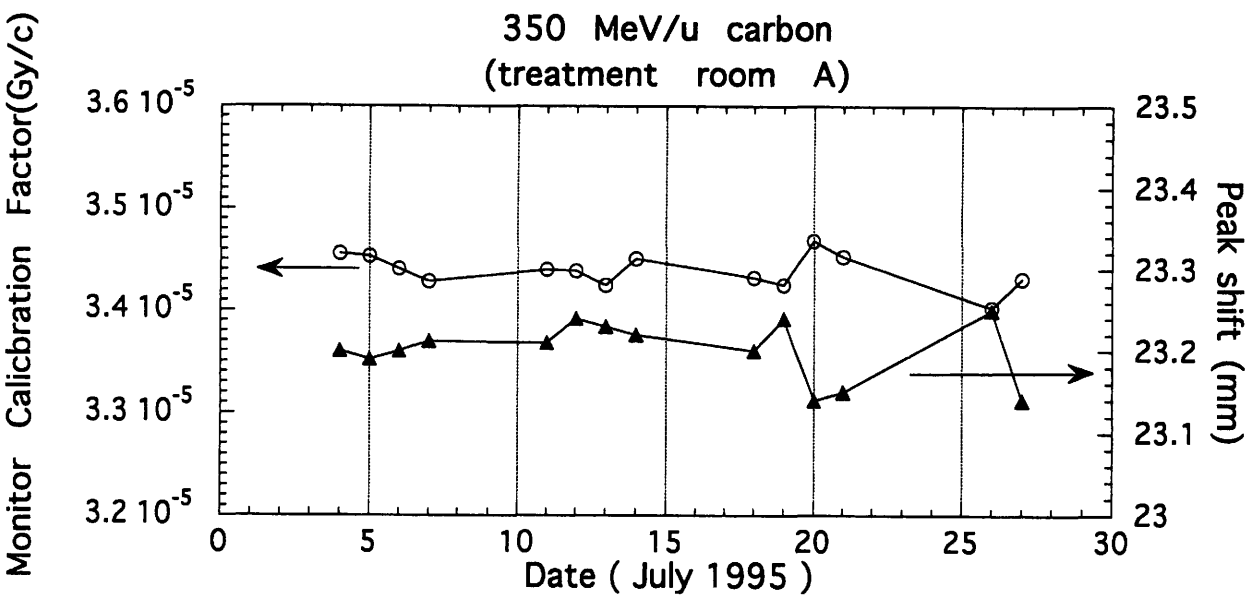

Fig. 2. Daily change of the monitor calibration factor and the peak shift

comparison with the calculation. The variation of the dose at 0 absorber position in the measurement of the depth dose distribution is also shown in the figure.

3) The information of the treatments, the excitation current of the wobbler magnets, thickness of the scatterer, sort of the ridge filter, thickness of the range shifter and so on, are send to the irradiation control computer. And the devices are adjusted according to the transferred information. The thickness of the binary filter is set so as for the residual range of the carbon beam to be half of the width of the spread-out Bragg peak. The standard chamber is set to the center of the spread-out Bragg peak, center of the target volume in the simulated phantom. Dose calibration of the monitor chamber is again performed under this treatment condition several times. These calibration factors are used for the real exposure to the patient.

4. Simplified Calibration

In the actual clinical trials, it takes about 30 minutes for taking the depth dose distribution, and about 5 minutes for taking each dose calibration factor of each patient. It takes an hour and half for the total calibration procedure of 12 patients. This calibration procedure is necessary whenever the initial energy of the carbon beam is changed. We use 290 and 350 or 400 MeV/u carbon beams in one day at HIMAC clinical trials. At that case, it takes 3 hours for the calibration. In order to shorten the calibration time, we are going to adapt a simplified calibration procedure from this autumn. The procedure is as follows;

1) The depth dose distribution is measured by a multi-layer ionization chambers in one exposure.

2) The dose calibration measurement for the each patient condition is performed only at the first treatment. The ratio of the dose calibration factor to the entrance dose of the depth dose distribution is recorded and used for the next treatments. The dose calibration factor for the later treatment is obtained by the ratio times the entrance dose of the depth dose distribution of that day.

From these simplified procedure of the dose calibration, it is possible to shorten the calibration time without making the accuracy of the dose calibration worse.

References

[1] Tujii, H., et al., XXI PTCOG meeting (1994).

[2] Kanai, T., et al., XXI PTCOG meeting (1994).

BEAM-QUALITY MEASUREMENTS ON HEAVY ION THERAPEUTIC BEAM OF HIMAC

Naruhiro MATSUFUJI, Tatsuaki KANAI, Hiromi TOMURA, Yasuyuki FUTAMI,
Akifumi FUKUMURA*, Toshiyuki KOHNO** and Kiyomitsu KAWACHI

Division of Accelerator Physics and Engineering, *Division of Radiation Research,
National Institute of Radiological Sciences, Chiba, Chiba, Japan
**Department of Energy Sciences, Tokyo Institute of Technology, Yokohama, Kanagawa, Japan

Abstract

Fluence spectra of fragment particles caused by spallation reactions between heavy ion beams and PMMA (polymethyl methacrylate; Lucite) target were measured with ΔE-E counter telescope method for each fragmented element. Measurements were carried out for carbon beams of 290 MeV/nucleon and 400 MeV/nucleon at Heavy Ion Medical Accelerator in Chiba (HIMAC), and 135 MeV/nucleon carbon beam at RIKEN Ring Cyclotron with changing the thickness of target material. Incident beam was broadened with a pair of wobbler magnets and a scatterer, in the same way of clinical trials which have been carrying out at HIMAC. Results were compared with the calculational expectations.

1. Introduction

In tumor therapy using heavy ion beams, it has been well known that incident heavy ion particles cause spallation reactions with the elements which compose the body. Hence, various kinds of particles were produced and hit the target. It is of importance to measure their fluence spectra for each fragmented element to estimate their influence on tumor therapy, and to brash up our treatment planning as well.

2. Experimental Setup

Figure 1 shows schematic diagrams of detector systems for measurements at RIKEN and HIMAC. According to Bethe formula, fragment particle can be identified with the parameter AZ^2 by measuring its total energy E and energy loss ΔE. The systems were based on the counter-telescope method [1]. Incident beam was sufficiently uniformed to 10.0 cm in diameter with the flatness of 95% at the iso-center by a pair of wobbler magnets and a scatterer[2]. A beam monitor, made of NE102A plastic scintillator of 1.5 cm in thickness, had front surface of 20.0 cm by 20.0 cm to count the total number of incident particles. The beam diameter was less than 5 cm at this beam monitor position. A stack of the plates of PMMA was selected as target material as it has similar composition with muscles. At the irradiation site, the detectors for the particle identification were placed. The detectors had comparatively smaller front surface to avoid entering plural fragment particles. In the setup at RIKEN, a coincidence detector, made of annular NE102A plastic scintillator, of 5.0 mm in diameter was positioned to distinguish an event by one fragment particle from those by noises. A proportional counter with tissue-equivalent gas was used to estimate the amount of energy transferred to biological system. A totally depleted silicon surface barrier detector of 11.3 mm in diameter and 1.0 mm in thickness was used as a ΔE counter to measure the energy loss ΔE in the detector and to make energy calibration. At the end of the beam line, a BGO scintillator was utilized as an E counter to measure the residual energy E of incident particle. The scintillator had a cylindrical form, 15.0 mm in diameter and 15.0 mm in length. The measurements were carried out for carbon 135 MeV/nucleon beam at E5 port.

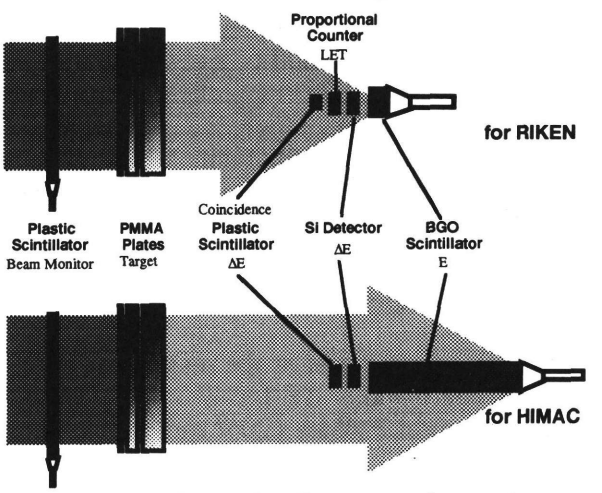

Fig. 1 The schematic diagram of the detector system.

In the setup at HIMAC, a NE102A plastic scintillator of 40.0 mm by 40.0 mm and 5.0 mm in thickness was used as a ΔE detector instead of Si semiconductor detector. Energy

resolution of plastic scintillator is generally inferior to semiconductor detector, however, scintillator has very superior characteristic on particle identification regarding that the response function of scintillator tends to enhance the difference of AZ^2 on lighter elements such as hydrogen or helium which are important to be well identified on this work, whereas the output of Si semiconductor detector is strictly proportional to AZ^2. In this setup, Si semiconductor detector was used for energy calibration. A larger BGO scintillator of rectangular form of 40.0 mm by 40.0 mm by 300.0 mm was used as an E detector. Measurements were carried out for carbon 290 and 400 MeV/nucleon beams at the bio port, therapy port BHC and CHC of the HIMAC.

3. Analysis

Figure 2 illustrates an example of particle identification by E-ΔE scatter plot obtained from incidence of carbon 290 MeV/nucleon beam to the target material of 120.7 mm in thickness. The abscissa represents the residual energy E measured by the BGO scintillator and the ordinate denotes the energy

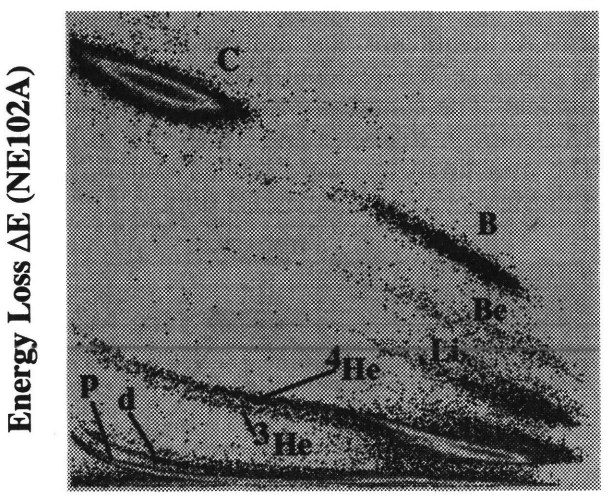

Fig. 2 The scatter plot of the residual energy E and the energy loss ΔE for 290 MeV/nucleon carbon beam in PMMA 120.7 mm in thickness.

loss ΔE from the plastic scintillator. Fragment particles were clearly separated to some groups.

To identify each group in the ΔE-E scatter plot, the amount of energy deposited in the Si semiconductor detector was compared with the calculational expectation for each fragmented element which was regarded on ΔE-E scatter plot as filled in Fig.2. Experimental energy deposition of each fragmented element was derived by picking up upper and lower channels of the distribution spectra on Si semiconductor detector. Here, the channel of Si semiconductor detector was calibrated by corresponding a peak channel of the group regarded as primary carbon with its amount of energy deposition calculated for each thickness of target material. As for calculational expectation of the energy deposition, maximum and minimum values were given by the fragment produced just before the detector and the fragment produced at an entrance of target material, respectively.

The result was summarized in Fig.3 for the incidence of 290 MeV/nucleon carbon beam in PMMA of 112.1 mm in thickness. The experimental and calculational range of deposited energy was well overlapped for each other on each fragmented element. Therefore, it can be said that fragment particles were clearly identified from carbon to hydrogen with the difference of Z and A by regarding the highest group as primary carbon in E-ΔE scatter plot.

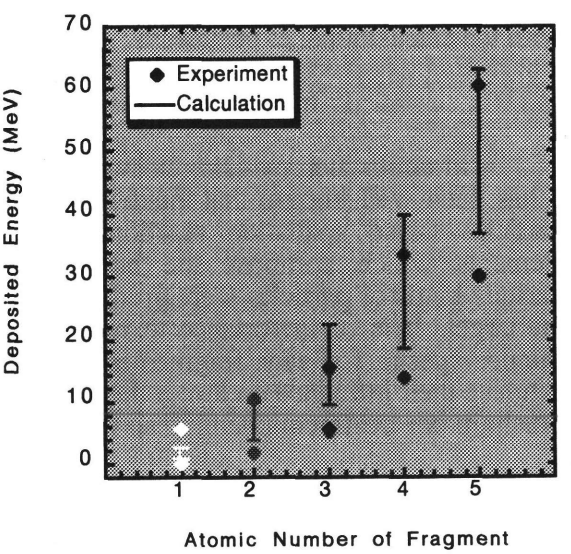

Fig.3 Experimental and calculational energy deposition on Si semiconductor detector for 290 MeV/nucleon carbon beam in PMMA of 112.1 mm in thickness.

Fluence spectra of each element were derived from the number of particles in each group by normalizing with the total number of incident particles because of the flatness and the broadness of the incident beam. Figure 4 to 6 displays the fluence spectra at the incidence of 135, 290 and 400 MeV/nucleon carbon beam respectively. In these figures, dots represents the results of this work and lines are

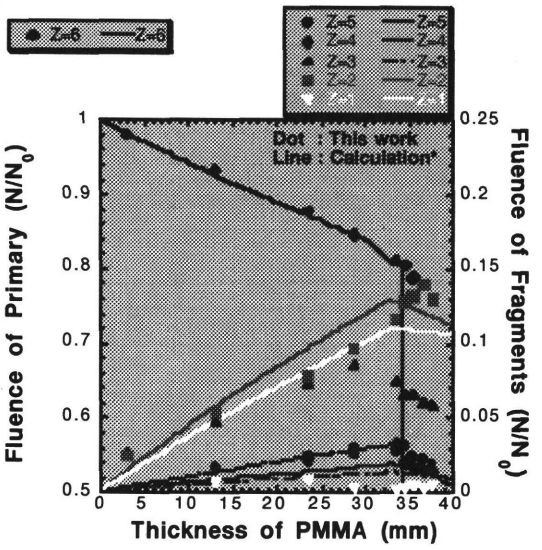

Fig.4 Fluence Spectra of fragments for 135 MeV/nucleon carbon beam.

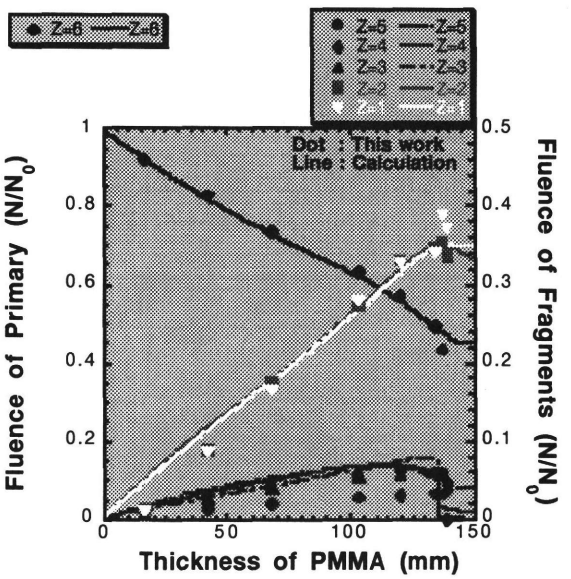

Fig.5 Fluence Spectra of fragments for 290 MeV/nucleon carbon beam.

calculational results by Sihver et al. [3] for the sake of comparison. The experimental data show good agreement with calculational ones.

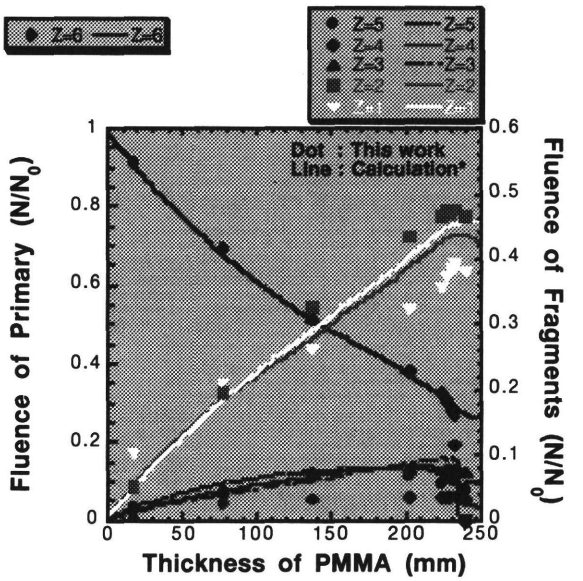

Fig.6 Fluence Spectra of fragments for 400 MeV/nucleon carbon beam.

4.Conclusion

Fragment particles included in the therapeutic beam were well identified with the ΔE-E scatter plot by a thin plastic scintillator and a BGO scintillator. The fluence spectra were obtained for each fragmented element and agreed well with the calculational expectations.

References

[1] F. S. Gelding and B. G. Harvey, Ann. Rev. Nucl. Sci. **25** (1975) 167

[2] T. R. Renner and W. T. Chu, Med. Phys. **14** (1987) 825

[3] L. Sihver et al., Proc. of NIRS Intl. Sem. on the Appl. of Heavy Ion Accel. to Rad. Therapy of Cancer in connection with XXI PTCOG Meeting, to be published.